ORNL/TM-10102
Distribution
Category UC-20c

METALS AND CERAMICS DIVISION

SECOND ANNUAL PROGRESS REPORT ON UNITED STATES-JAPAN COLLABORATIVE TESTING IN THE HIGH FLUX ISOTOPE REACTOR AND THE OAK RIDGE RESEARCH REACTOR FOR THE PERIOD ENDING SEPTEMBER 30, 1985

J. L. Scott, M. L. Grossbeck, L. K. Mansur, A. F. Rowcliffe,
I. I. Siman-Tov, and K. R. Thorns
Oak Ridge National Laboratory

and

M. P. Tanaka, S. Hamada, T. Kondo, and A. Hishinuma
Japan Atomic Energy Research Institute
Tokai-mura, Japan

Date Published - August 1986

Prepared for
Office of Fusion Energy

Prepared by the
OAK RIDGE NATIONAL LABORATORY
Oak Ridge, Tennessee 37831
operated by
MARTIN MARIETTA ENERGY SYSTEMS, INC.
for the
U.S. DEPARTMENT OF ENERGY
under Contract No. DE-AC05-84OR21400

MARTIN MARIETTA ENERGY SYSTEMS LIBRARIES

3 4456 0069952 7

Printed in the United States of America. Available from
National Technical Information Service
U.S. Department of Commerce
5285 Port Royal Road, Springfield, Virginia 22161
NTIS price codes—Printed Copy: A04; Microfiche A01

This report was prepared as an account of work sponsored by an agency of the United States Government. Neither the United States Government nor any agency thereof, nor any of their employees, makes any warranty, express or implied, or assumes any legal liability or responsibility for the accuracy, completeness, or usefulness of any information, apparatus, product, or process disclosed, or represents that its use would not infringe privately owned rights. Reference herein to any specific commercial product, process, or service by trade name, trademark, manufacturer, or otherwise, does not necessarily constitute or imply its endorsement, recommendation, or favoring by the United States Government or any agency thereof. The views and opinions of authors expressed herein do not necessarily state or reflect those of the United States Government or any agency thereof.

CONTENTS

ACKNOWLEDGMENTS v
LIST OF FIGURES vii
LIST OF TABLES ix
ABSTRACT 1
1. INTRODUCTION 1
1.1 BACKGROUND 1
1.2 OBJECTIVES 2
1.3 SCOPE 2
2. HFIR CAPSULES 2
2.1 PROGRESS AND STATUS 2
2.2 POSTIRRADIATION EXAMINATION OF CAPSULE JP-1 4
2.3 POSTIRRADIATION EXAMINATION OF CAPSULE JP-3 9
2.4 HFIR TEMPERATURE EXPERIMENT 10
2.5 TEM EXAMINATION OF JPCA AND J316 ALLOYS FROM CAPSULE JP-1 . 15
3. ORR SPECTRAL-TAILORING EXPERIMENTS 18
3.1 EXPERIMENT OBJECTIVES 19
3.1.1 Irradiation Creep 21
3.1.2 Embrittlement 22
3.1.3 Microstructure 23
3.1.4 Ceramics 24
3.1.5 Objective of the HEDL Test Matrix 24
3.1.6 Objectives of the JAERI Program 25
3.2 TEST MATRIX 26
3.3 PRESSURIZED TUBES 26
3.4 TENSILE SPECIMENS 32
3.5 FATIGUE SPECIMENS 32
3.6 CRACK-GROWTH SPECIMENS 35
3.7 TEM DISKS 43
3.8 CAPSULE ASSEMBLY 46
3.9 CAPSULE OPERATION 53
4. CONCLUSIONS. 53
5. REFERENCES 55

BLANK PAGE

ACKNOWLEDGMENTS

The authors of this report would like to acknowledge the help of Dr. T. C. Reuther, DOE, and E. Shirai, JAERI, who serve on the Steering Committee and have provided much support in the creation and implementation of this collaboration. The authors would also like to thank Frances Scarboro and Bertie Byrum for preparing the draft of this report and D. L. Northern of the Metals and Ceramics Division Publications Office for final preparation.

BLANK PAGE

LIST OF FIGURES

Figure	Legend	Page
2.1	HFIR-JP irradiation schedule	3
2.2	Postirradiation examination schedule for JP capsules (typical)	4
2.3	JP-1 capsule mounted in a chuck prior to making the first cut	5
2.4	JP-1 specimen holders during capsule disassembly	7
2.5	Hourglass fatigue specimens and TEM holder after removal from JP-1	7
2.6	Submini tensile specimens after removal from JP-1	7
2.7	General arrangement of core target tower and quick access hatch	11
2.8	RB and proposed RB* positions	12
2.9	HFIR target region with two capsules	13
2.10	Proposed configuration for the target temperature test capsule	14
2.11	Cavity microstructure of *(a)* JPCA-SA and *(b)* J316-SA after irradiation in HFIR to 30 dpa	16
2.12	Distribution of MC precipitates in JPCA-20% CW after irradiation in HFIR to 30 dpa at 300°C	18
3.1	Cross section of the MFE-6J capsule with typical test specimen locations	20
3.2	Pressurized tube design; all dimensions are in millimeters	32
3.3	SS-l tensile specimen	34
3.4	SS-3 tensile specimen	34
3.5	HFIR submini tensile specimen	35
3.6	Grodzinski fatigue specimen	40
3.7	Hourglass fatigue specimen; all dimensions are in millimeters	40
3.8	Crack-growth specimen; tabs are welded along the 25.4-mm edge following irradiation	42
3.9	ORR spectral-tailoring capsule MFE-7J specimens prior to assembly.	51
3.10	ORR spectral-tailoring capsule MFE-7J specimen assembly	52

BLANK PAGE

LIST OF TABLES

Table	Legend	Page
2.1	Displacements per atom and helium contents in HFIR-JP-1 capsule.	3
2.2	Displacements per atom and helium contents in HFIR JP-3 capsule.	4
2.3	Length changes of submini tensile specimens in HFIR JP-1 capsule.	9
2.4	Immersion densities of submini tensile specimens	9
2.5	Length changes of submini tensile specimens in HFIR JP-3 capsule.	10
2.6	Heat and mechanical treatment	15
2.7	Cavity data for JPCA and J316 stainless steels irradiated in HFIR.	17
2.8	Dislocation parameters for JPCA and J316 stainless steels irradiated in HFIR	17
3.1	Ceramics being irradiated in capsules MFE-6J and -7J	24
3.2	Test matrix for the MFE-6J and -7J capsules	27
3.3	Alloys in the ORNL test matrix for the MFE-6J and -7J capsules	28
3.4	Alloys in the HEDL test matrix for the MFE-6J and -7J capsules	30
3.5	Alloys in the JAERI test matrix for the MFE-6J and -7J capsules	31
3.6	Test matrix for pressurized tubes in MFE-6J and -7J capsules	33
3.7	ORNL SS-1 tensile test matrix in MFE-6J and -7J capsules	36
3.8	Test matrix of ORNL SS-3 tensile specimens in MFE-6J and -7J capsules	37
3.9	Test matrix of HEDL SS-3 tensile specimens in MFE-6J and -7J capsules	38
3.10	JAERI tensile test matrix in MFE-6J and -7J capsules	39
3.11	JAERI fatigue test matrix in MFE-6J and -7J capsules	41
3.12	Test matrix of HEDL crack-growth specimens in MFE-6J capsule.	42

Table	Legend	Page
3.13	Description of JAERI crack-growth specimens in MFE-6J and -7J capsules	43
3.14	Test matrix of TEM disk packets in MFE-6J and -7J capsules	44
3.15	ORNL TEM matrix for MFE-6J and -7J capsules	45
3.16	HEDL TEM matrix for MFE-6J	46
3.17	HEDL TEM matrix for MFE-7J	47
3.18	JAERI engineering alloy TEM matrix in MFE-6J and -7J	49
3.19	JAERI basic research TEM test matrix in MFE-6J and -7J	50
3.20	Operating data for the ORR-MFE-6J and -7J experimental capsules as of September 30, 1985	54

SECOND ANNUAL PROGRESS REPORT ON UNITED STATES-JAPAN COLLABORATIVE TESTING IN THE HIGH FLUX ISOTOPE REACTOR AND THE OAK RIDGE RESEARCH REACTOR FOR THE PERIOD ENDING SEPTEMBER 30. 1985*

J. L. Scott, M. L. Grossbeck, L. K. Mansur, A. F. Rowcliffe, I. I. Siman-Tov, K. R. Thorns, M. P. Tanaka,† S. Hamada,† T. Kondo,‡ and A. Hishinuma‡

ABSTRACT

The second year of the program of U.S.-Japan collaborative testing in the HFIR and ORR has been successfully completed. Two of eight phase-I HFIR target capsules were irradiated, and postirradiation testing was begun. Two spectral-tailoring capsules, MFE-6J and -7J, were fabricated and installed in the ORR. The JEOL JEM 2000FX microscope was installed at ORNL and is now being operated routinely. Microstructural data of the JPCA in the SA, 10%, and 20% cold-worked conditions and type J316 in the SA and 20% cold-worked conditions reveal that all specimens examined clearly show a high concentration of fine helium bubbles after irradiation to about 30 dpa at 300°C (in HFIR). Precipitation of MC was observed in 20% cold-worked JPCA. Swelling of all specimens was less than 1%.

1. INTRODUCTION

1.1 BACKGROUND

This report covers the second year of a five-year program of U.S.-Japan collaborative testing in the High Flux Isotope Reactor (HFIR) and the Oak Ridge Research Reactor (ORR). In last year's annual report[1] the implementing agreement, the objective and scope, and the facilities being used were discussed in detail. This report describes the status of the

*Research sponsored by the Office of Fusion Energy, U.S. Department of Energy, under Contract No. DE-AC05-84OR21400 with Martin Marietta Energy Systems, Inc.

†Japan Atomic Energy Research Institute, Tokai-mura, Japan, assigned to ORNL.

‡Japan Atomic Energy Research Institute, Tokai-mura, Japan.

HFIR capsules, presents preliminary postirradiation examination results on the first capsules to be completely irradiated, and gives a full description of the test matrix and assembly of the ORR capsules. It is a requirement of the collaboration agreement that an annual report be issued.

1.2 OBJECTIVES

The objectives of the program are to (1) design, conduct, and evaluate joint irradiation experiments in the HFIR and ORR; (2) investigate the response of Japanese and U.S. structural alloys to high levels of displacements per atom (dpa) and helium content in the HFIR; and (3) investigate the response of U.S. and Japanese prime-candidate alloys (PCA and JPCA) to the correct helium-to-dpa ratio in the ORR. With the recent change in emphasis of the U.S. fusion program to longer-range problems, a secondary U.S. objective is to study basic radiation processes under well-controlled conditions.

1.3 SCOPE

The scope of the program consists of eight phase-I HFIR target capsules to be irradiated to exposures between 30 and 50 dpa at temperatures in the range 300 to 600°C, and two ORR spectral-tailoring capsules to be irradiated to 30 dpa, with interim examinations at 10 and 20 dpa. Each ORR capsule provides two different irradiation temperatures, thus specimens are being irradiated at 60, 200, 330, and 400°C. The program includes eight phase-II HFIR capsules scheduled to be planned in FY 1986.

The status of the eight phase-I HFIR capsules and the two ORR capsules is described in the following sections.

2. HFIR CAPSULES

2.1 PROGRESS AND STATUS

A description of the HFIR phase-I capsules and the complete test matrix was reported previously.[1] Two capsules, JP-1 and -3, have completed irradiation, and six capsules are still in the reactor. The

present irradiation schedule is shown in Fig. 2.1. Damage levels achieved by the specimens in the JP-1 and -3 capsules are given in Tables 2.1 and 2.2. The specimen descriptions and compositions were reported previously.[1]

ORNL-DWG 86-8463

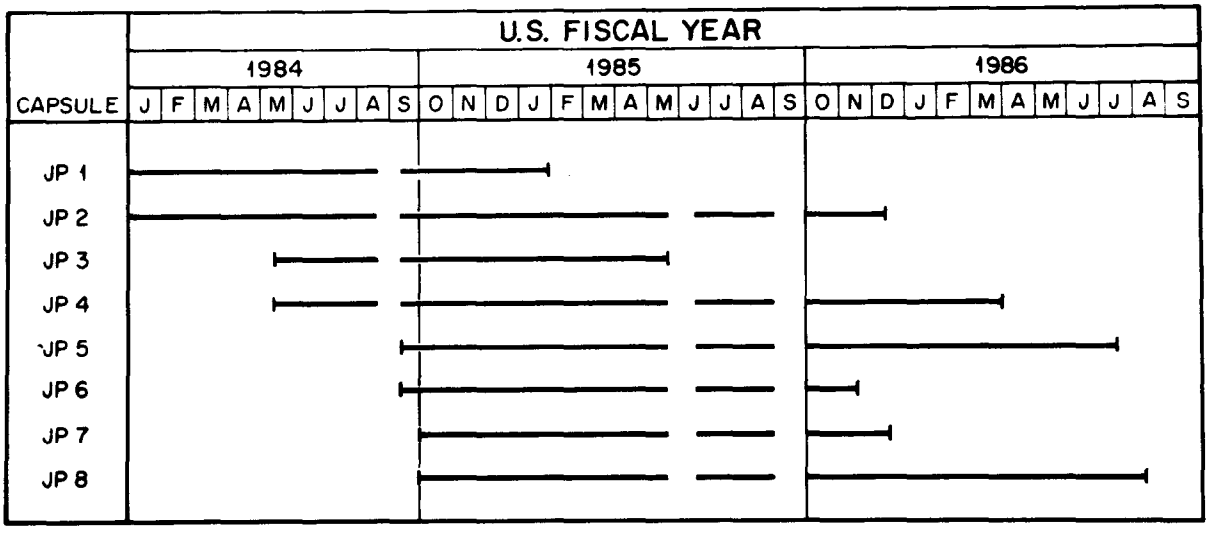

Fig. 2.1. HFIR-JP irradiation schedule.

Table 2.1. Displacements per atom and helium contents in HFIR-JP-1 capsule[a]

Position	Distance from HFIR centerline (cm)	Temperature (°C)	Alloy	Specimen type	Identification	Displacements per atom (dpa)	Helium content (at. ppm)
1	23.20	300	PCA	Tensile	EL15	15.82	1014
2	18.76	400	PCA	Tensile	EL21	22.06	1546
3	14.31	500	PCA	Tensile	EL28	26.97	1964
4	9.59	430	316	Fatigue	AA1	29.97	1843
5	4.58	430	316	Fatigue	AA2	32.24	1999
6	0.00	300	J316[b]	TEM disks		33.03	2116
7	4.58	430	JPCA	Fatigue	FE1	32.93	2417
8	9.59	430	JPCA	Fatigue	FE2	30.60	2230
9	14.31	500	JPCA	Tensile	TB1	26.87	1925
10	18.76	400	JPCA	Tensile	TB2	21.98	1520
11	23.20	300	JPCA	Tensile	TE1	15.77	1004

[a]MWd = 33,644; removed from HFIR February 1, 1985.

[b]This holder contained several alloys.

Table 2.2. Displacements per atom and helium contents in HFIR JP-3 capsule[a]

Position	Distance from HFIR centerline (cm)	Temperature (°C)	Alloy	Specimen type	Identification	Displacements per atom (dpa)	Helium content (at. ppm)
1	23.20	300	PCA	Tensile	EL30	16.00	1020
2	18.76	400	PCA	Tensile	EL34	22.32	1559
3	14.31	500	PCA	Tensile	EC29	27.28	1981
4	9.59	430	316	Fatigue	EC152	31.07	2298
5	4.58	430	316	Fatigue	AA8	32.60	2019
6	0.00	300	J316[b]	TEM disks		33.40	2142
7	4.58	430	JPCA	Fatigue	FE5	33.30	2447
8	9.59	430	JPCA	Fatigue	FE6	30.95	2258
9	14.31	500	JPCA	Tensile	TB7	27.17	1950
10	18.76	400	JPCA	Tensile	TB8	22.23	1541
11	23.20	300	JPCA	Tensile	TB9	15.95	1019

[a]MWd = 34,019; removed from HFIR May 28, 1985.

[b]This holder contained several alloys.

2.2 POSTIRRADIATION EXAMINATION OF CAPSULE JP-1

The steps in postirradiation examination (PIE) and a typical schedule are shown in Fig. 2.2. The upper and lower ends of capsule JP-1 were removed with an abrasive cut-off wheel, as shown in Fig. 2.3. The inner

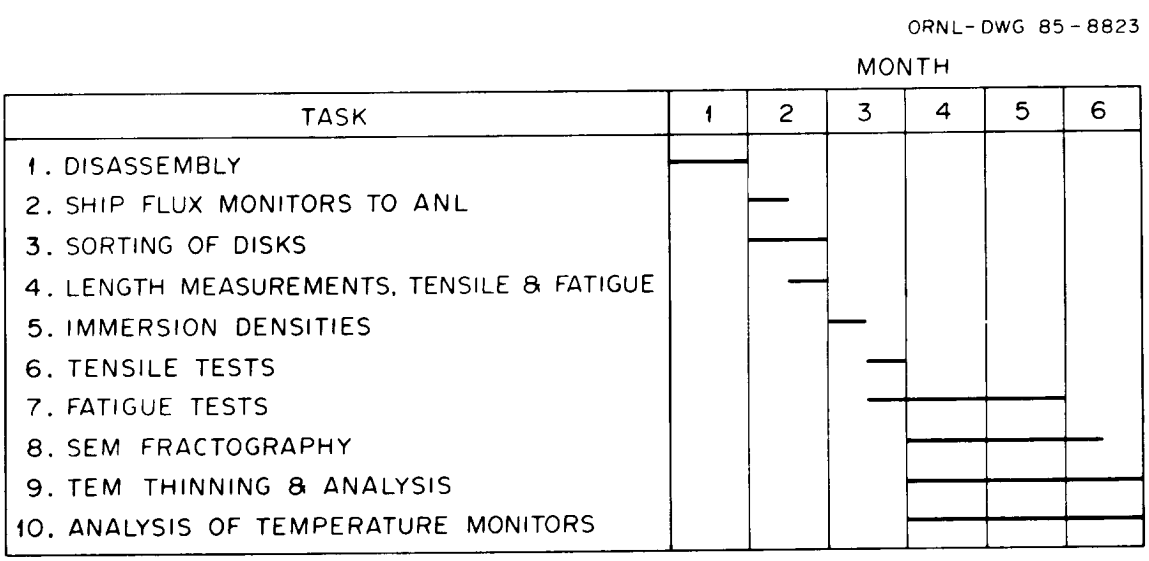

Fig. 2.2. Postirradiation examination schedule for JP capsules (typical).

YP004

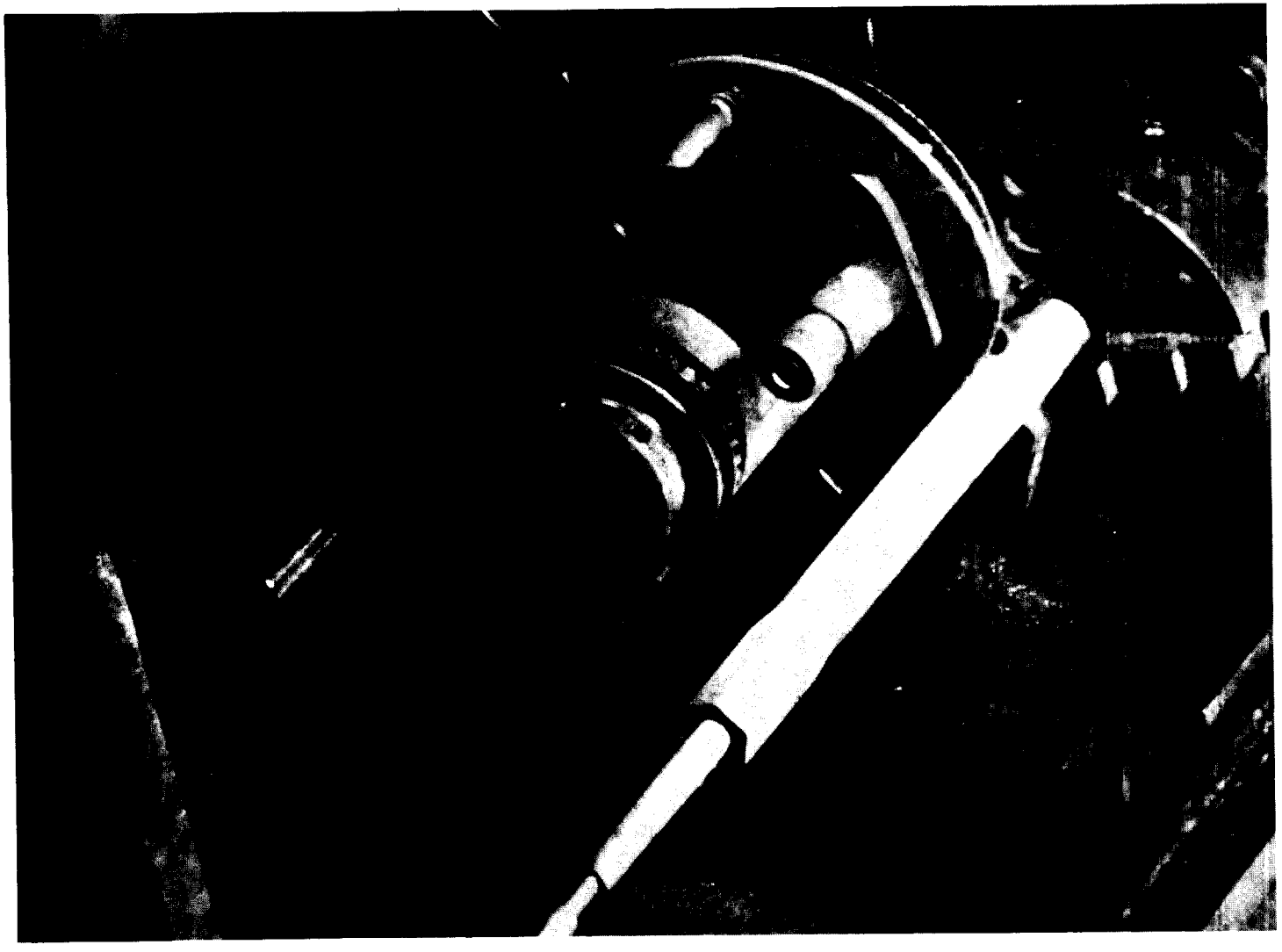

Fig. 2.3. JP-1 capsule mounted in a chuck prior to making the first cut.

and outer containment were cut axially the entire length and removed. The appearance of the specimen holders is shown in Fig. 2.4; all areas were bright and shiny, indicating no water leakage into the capsule. The flux monitors located at the top of holders 3, 5, 6, 9, and 11 were identified and shipped to L. R. Greenwood of the Argonne National Laboratory for analysis. Specimens (Figs. 2.5 and 2.6) were removed from their holders by cutting the retainer rings and prying apart the half shells.

Figure 2.5 shows the four hourglass fatigue specimens and the holder containing transmission-electron-microscopy (TEM) disks. The holder was irradiated at 300°C, whereas all fatigue specimens were irradiated at 430°C. There was a slight discoloration of the fatigue specimens because of surface oxidation. Even though the capsule is filled with helium, some outgassing occurs during the initial heatup in the reactor, leading to superficial oxidation at the higher specimen temperature. Somewhat greater oxidation was observed on tensile specimens irradiated at 500°C (Fig. 2.6). The two center specimens were irradiated at 500°C. Specimens irradiated at 400°C (next to the 500°C specimens) and those irradiated at 300°C were bright and shiny following the experiment.

Swelling was determined using two methods: length and immersion density measurement. The two methods serve as checks on each other, but the immersion density method is more precise for such small specimens, since it has a limit of error of about ±0.2% change in density. Length measurements are listed in Table 2.3; all values are small, probably at or below the level of sensitivity of the measurement. Immersion density measurements were made on the specimens following removal of the end spurs, which were irradiated at a lower temperature. Measurements were made on irradiated and unirradiated specimens in the same batch to obtain accurate differences in density between those irradiated and unirradiated. The results appear in Table 2.4. Again the values are small, but the highest swelling values correspond to the highest temperatures. Since these swelling values (0.5 and 0.3%) are outside the limit of error of 0.2%, they are considered value numbers, indicating very low and probably insignificant swelling.

In other hot-cell work the TEM disks have been sorted, and equipment is being prepared for tensile and fatigue testing.

YP001

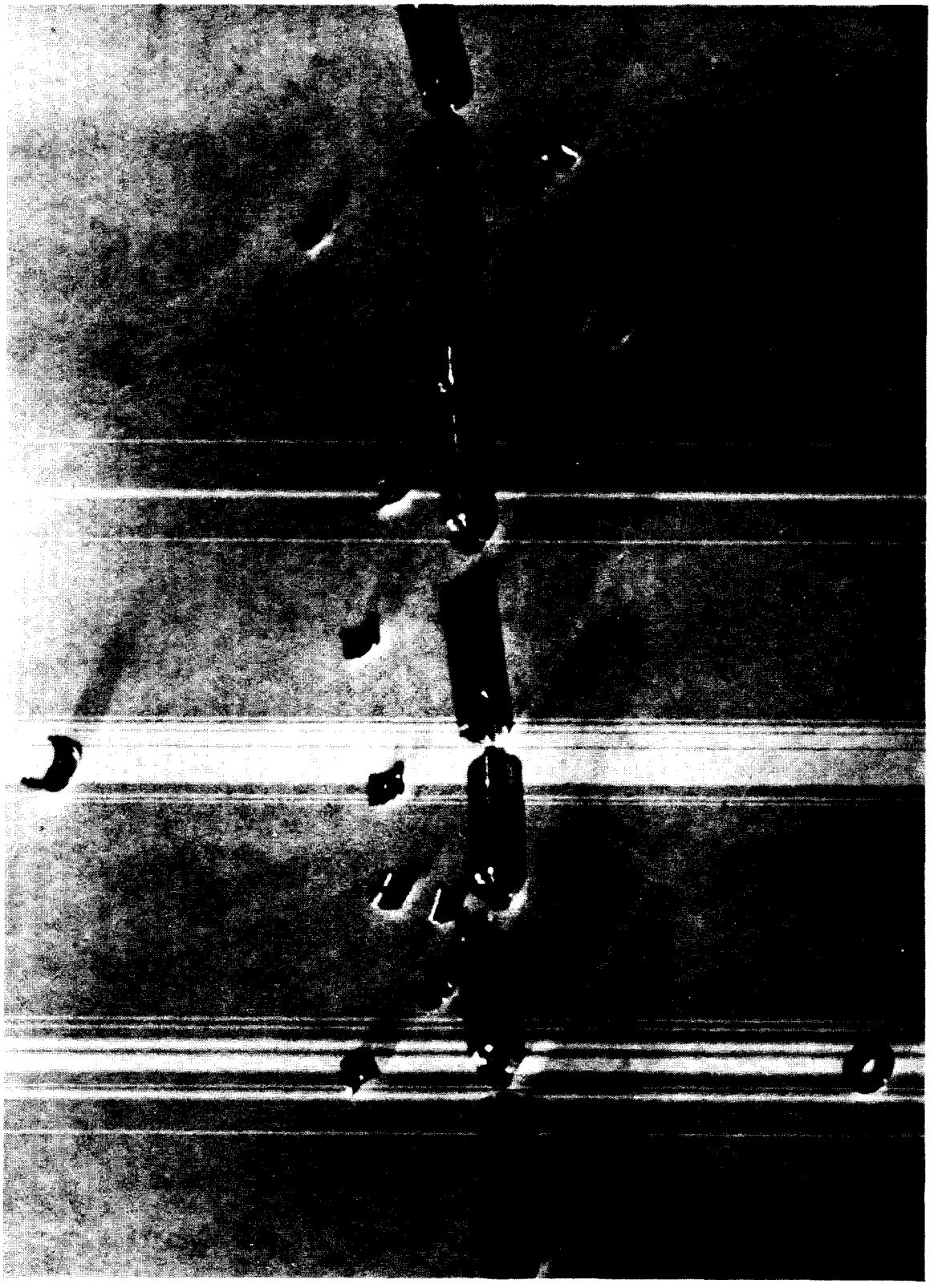

Fig. 2.4. JP-1 specimen holders during capsule disassembly.

YP005

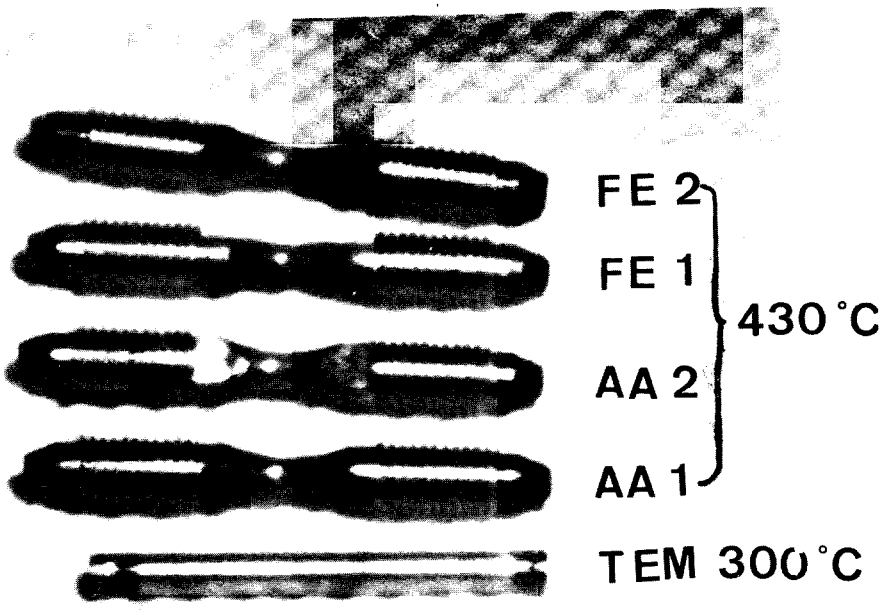

Fig. 2.5. Hourglass fatigue specimens and TEM holder after removal from JP-1.

YP006

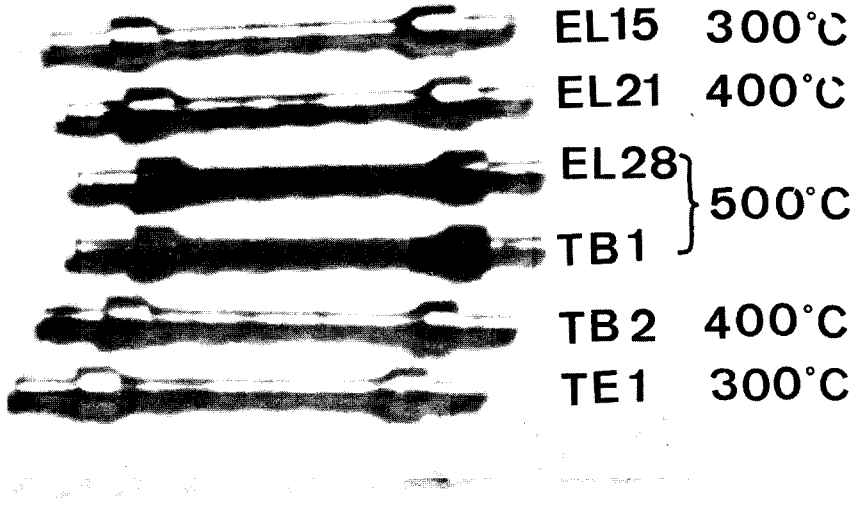

Fig. 2.6. Submini tensile specimens after removal from JP-1.

Table 2.3. Length changes of submini tensile specimens in HFIR JP-1 capsule

Specimen number	Alloy	Condition[a]	Irradiation temperature (°C)	Length (mm)		Increase (%)	$\frac{\Delta V}{V} = \frac{3\Delta L}{L}$
				Initial	Final		
EL15	PCA	B3	300	39.34	39.35	0.02	0.06
EL21	PCA	B3	400	39.34	39.46	0.31	0.93
EL28	PCA	B3	500	39.34	39.47	0.33	0.99
TB1	JPCA	PS2	500	39.39	39.50	0.28	0.84
TB2	JPCA	PS2	400	39.38	39.48	0.25	0.75
TE1	JPCA	PC2	300	39.37	39.46	0.23	0.69

[a]B3 = SA at 1100°C + 8 h at 800°C + 25% CW. PS2 = SA at 1100°C. PC2 = PS2 + 15% CW.

Table 2.4. Immersion densities of submini tensile specimens

Specimen number	Irradiation temperature (°C)	$\frac{\Delta V}{V_0} \left(= \frac{\Delta \rho}{\rho_f}\right)$ (%)
ELA[a]		0
EL15	300	0.013
EL21	400	0.070
EL28	500	0.496
TB13[a]		0
TB1	500	0.302
TB2	400	0.117
TE13[a]		0
TE1	300	0.072

[a]Control.

2.3 POSTIRRADIATION EXAMINATION OF CAPSULE JP-3

Capsule JP-3 has also been disassembled. The specimens had the same appearance as those in capsule JP-1. Length measurements of tensile specimens are shown in Table 2.5. Testing was interrupted following the length measurements.

Table 2.5. Length changes of submini tensile specimens in HFIR JP-3 capsule

Specimen number	Alloy	Condition[a]	Irradiation temperature (°C)	Length (mm)		Increase (%)
				Initial	Final	
EL30	PCA[b]	B3	300	39.34	39.39	0.14
EL34	PCA	B3	400	39.34	39.52	0.47
EC29	PCA	A3	500	39.35	39.43	0.20
TB7	JPCA[c]	PS2	500	39.41	39.45	0.10
TB8	JPCA	PS2	400	39.40	39.46	0.15
TB9	JPCA	PS2	300	39.40	39.43	0.08

[a]A3 = SA at 1100°C + 25% CW. B3 = SA at 1100°C + 8 h at 800°C + 25% CW. PS2 = SA at 1100°C.

[b]Prime candidate alloy.

[c]Japanese prime candidate alloy.

2.4 HFIR TEMPERATURE EXPERIMENT

An experiment in the U.S.-Japan collaborative testing program was evaluated to determine the temperatures in the HFIR target capsule. Originally this experiment was to be a passive one in which the thermal expansion of a gamma heat source would be measured accurately. The principal limitation to this method is that only a peak temperature at some point in the reactor cycle would be measured; therefore, an active experiment, such as one using thermocouples, was desired.

The opportunity for an active experiment became available when ORNL management decided to upgrade the HFIR to improve its capability for materials irradiation testing. In particular, it was decided to instrument two target-rod positions in the HFIR target and to enlarge and upgrade positions in the removable beryllium region [called RB star (RB*) position] just outside the reactor core. One can get an understanding of the HFIR modifications by studying the general arrangement of the new target tower and quick access hatch shown in Fig. 2.7. In order to instrument the target region, a new target tower and quick access hatch are required. The new hatch will contain two penetrations for instrumentation and a third penetration for a "rabbit tube," used in the manufacture of medical isotopes. In addition, there are eight penetrations that

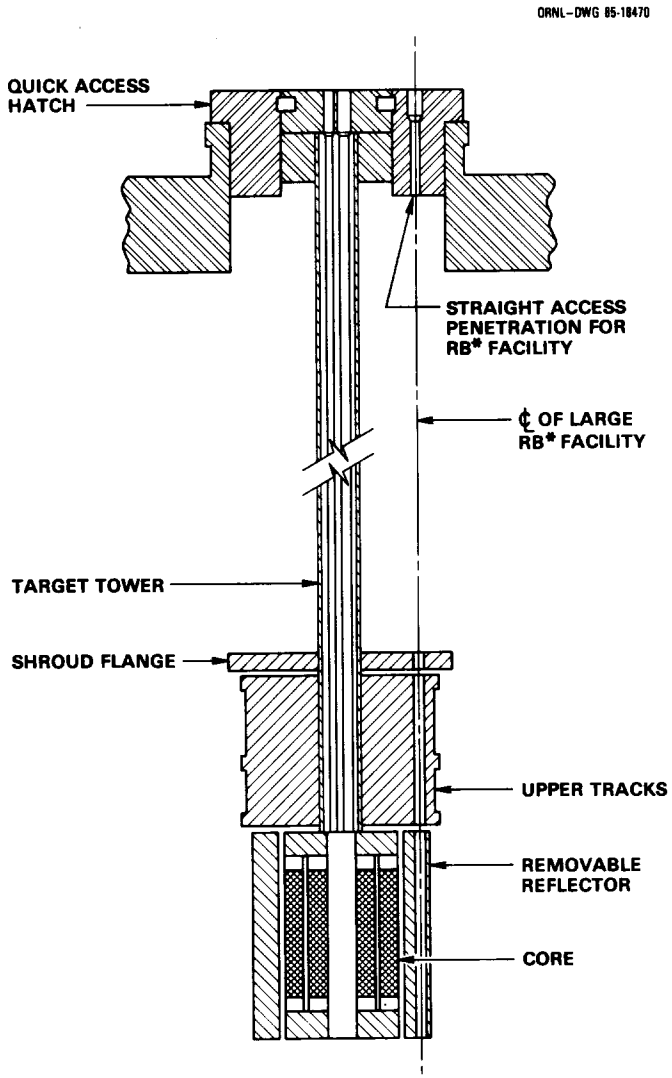

Fig. 2.7. General arrangement of core target tower and quick acce hatch.

provide straight access for the RB* positions. This access allows one to rotate the RB* capsules to provide a uniform fluence to all specimens, even though there is a flux gradient across the capsule.

The locations of the new RB* positions (viewed from above) are shown in Fig. 2.8. The left diagram shows the present HFIR core with four 33-mm die RB positions; the right side shows the new arrangement with the eight RB* positions. Modifications to the shroud flange and the upper tracks of the control plate assembly are required to complete the HFIR modification.

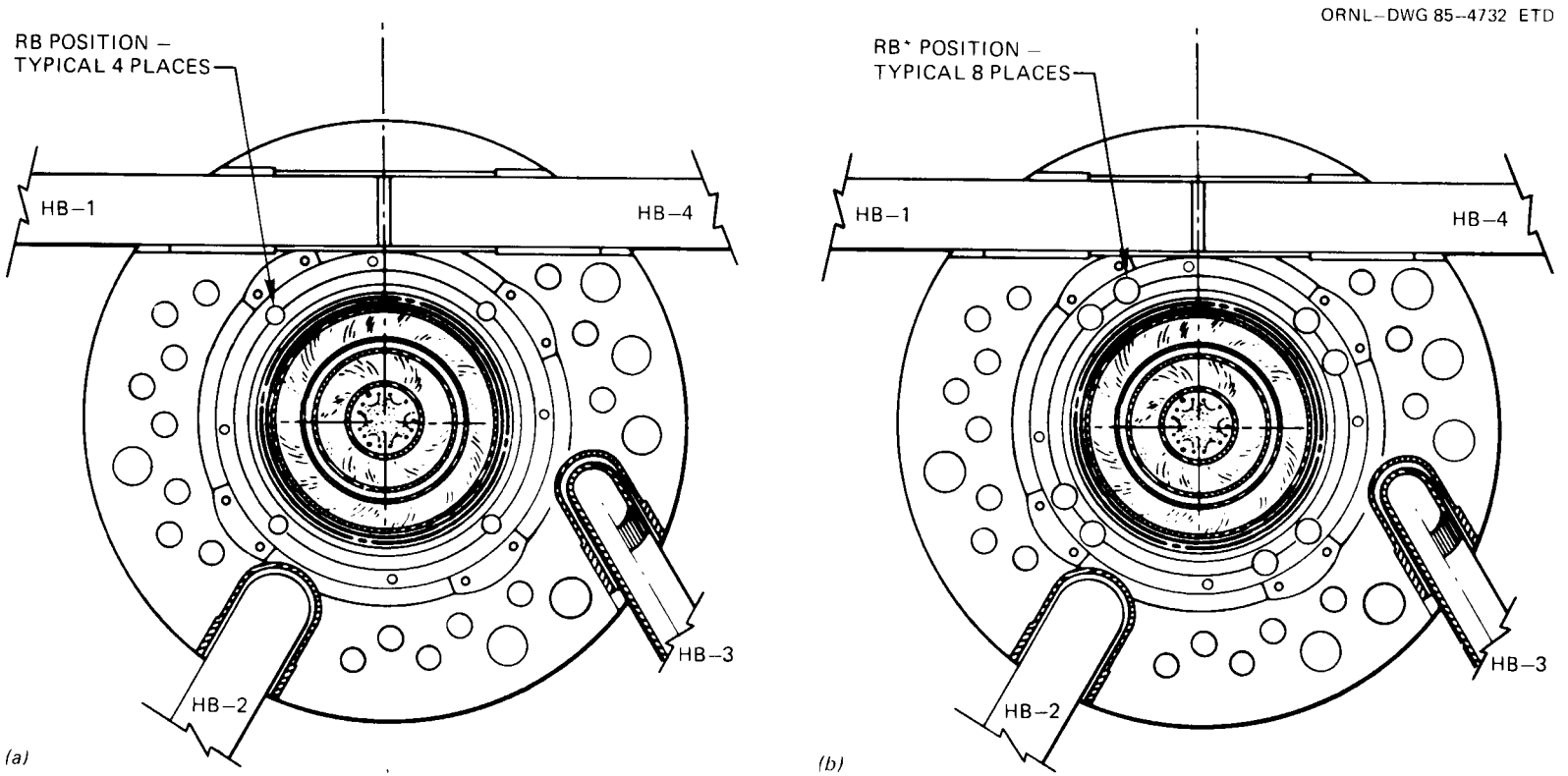

Fig. 2.8. RB and proposed RB* positions.

Further details of the new target region access hatch are shown in Fig. 2.9. The two instrument penetrations are shown together with a conceptual representation of how one might perform gamma shielding or spectral tailoring of an instrumented target capsule by replacing seven target rods with a capsule shroud of tungsten, cadmium, or hafnium. With somewhat reduced shielding, a 25.4-mm-diam (1.0 in.) capsule could be irradiated. No shielding is planned for the U.S.-Japan instrumented target capsule.

The proposed configuration for the U.S.-Japan target temperature test capsule is shown in Fig. 2.10. Typical tensile, fatigue, and TEM specimens will be produced with 1.016-mm-diam holes through which will pass a multifunction thermocouple. Specimen holders and helium gaps will be identical to those used in the JP–1 through JP-8 capsule series. The capsule will be operated in the HFIR for one or more cycles to obtain the temperature history for a given cycle and to determine the reproducibility between cycles. The schedule calls for this experiment to begin in August 1986.

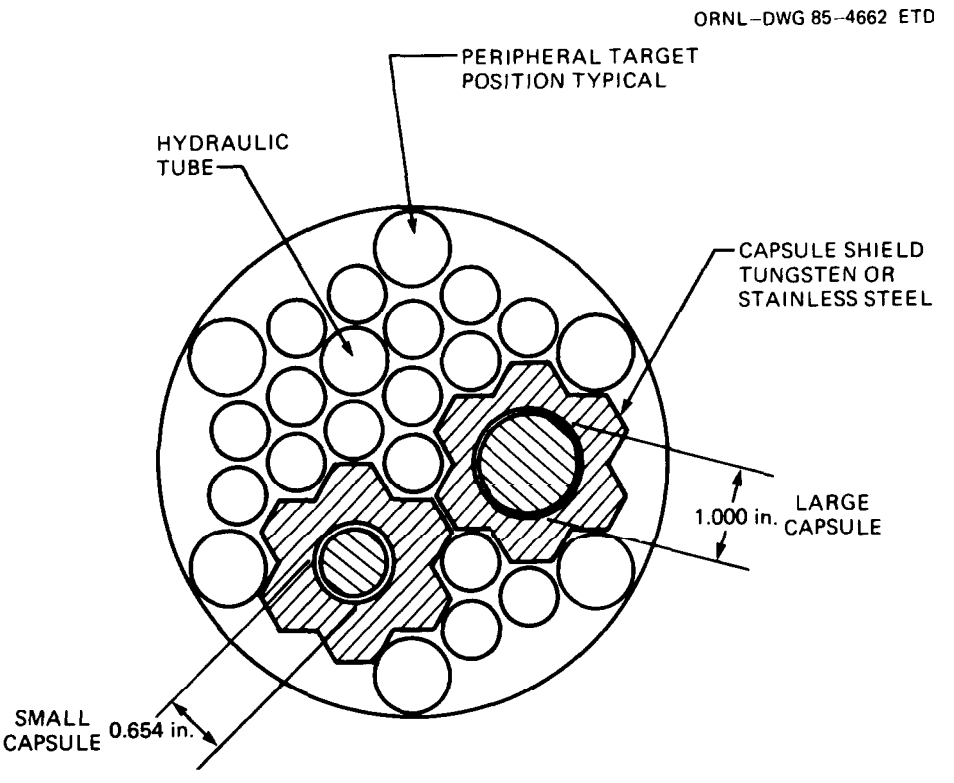

Fig. 2.9. HFIR target region with two capsules.

ORNL-DWG 86-1910

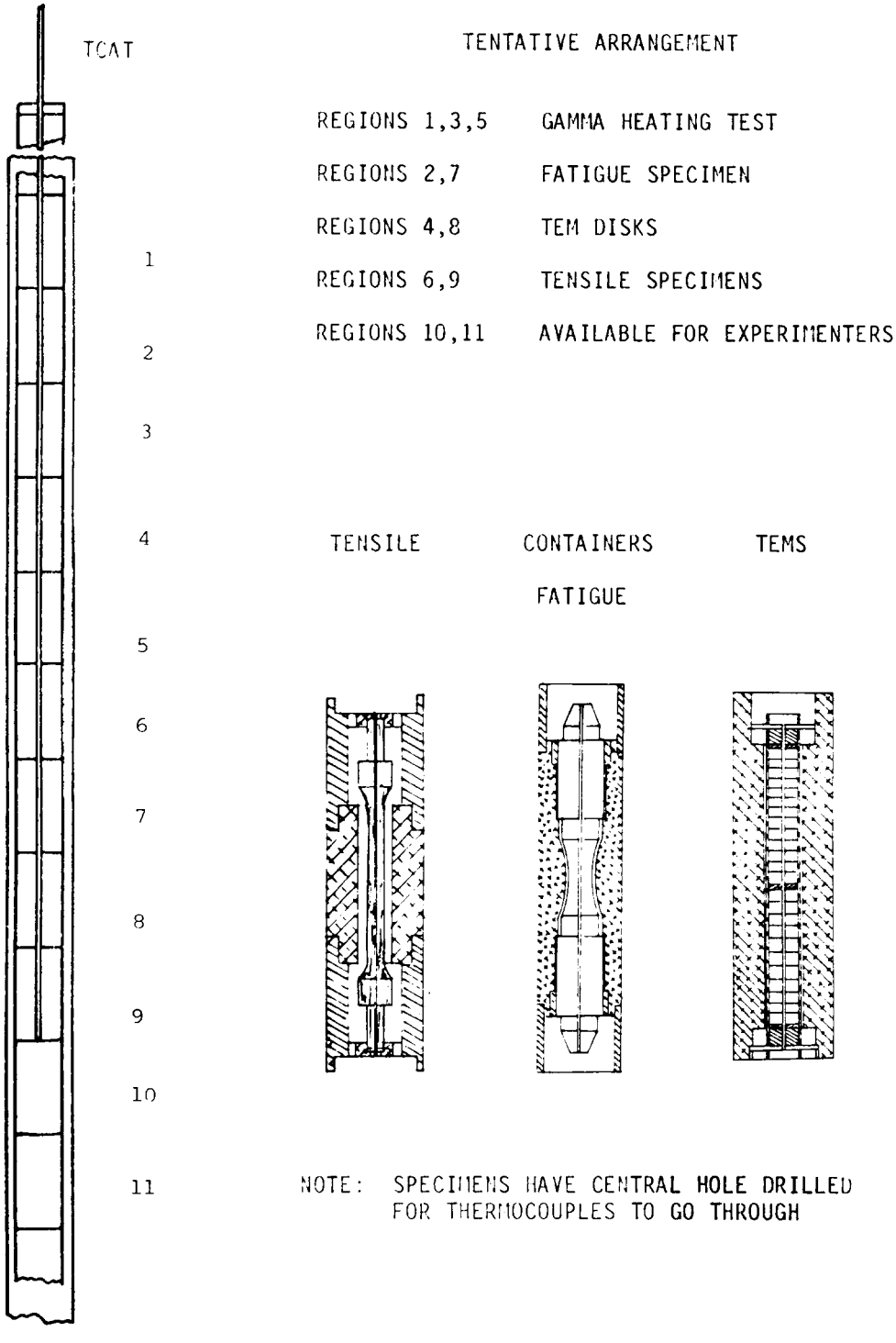

Fig. 2.10. Proposed configuration for the target temperature test capsule.

2.5 TEM EXAMINATION OF JPCA AND J316 ALLOYS FROM CAPSULE JP-1

The first HFIR specimens to be examined by electron microscopy were the Japanese prime candidate alloy (JPCA) and Japanese 316 stainless steels irradiated at 300°C in the JP-1 capsule. The chemical compositions of the two alloys are given in this report (see Table 3.5). Heat and mechanical treatments are presented in Table 2.6. The final thickness of all sheets was 0.254 mm. The 3-mm-diam disks were punched out from the sheet and irradiated at 300°C for 16 cycles (~8000 h) to 33,644 MWd in the JP-1 capsule. Displacement damage and helium content in JPCA and J316 produced 34.0 dpa and 2500 at. ppm, and 33.0 dpa and 2100 at. ppm, respectively. After irradiation, disks for transmission electron microscopy were thinned with a twin-jet Tenupol unit and examined using JEM 100CX and 2000FX electron microscopes.

Small cavities were observed in the microstructure of all JPCA solution-annealed (SA) and J316 (SA) specimen materials (Fig. 2.11). In all specimens, fine cavities of high concentration were quite uniformly dispersed throughout the matrix. Quantitative data on cavities are given in Table 2.7. The ratios of helium concentration for materials calculated from cavity microstructure to those produced by transmutations are listed in Table 2.7. The high ratio suggests that most of the observed cavities may be equilibrium helium bubbles; certainly they are not voids.

The dislocation structure of all specimens consisted of a heavy concentration of networks and Frank-faulted loops. Frank-faulted loops were imaged separately from the network using a high-resolution dark field with <111> kinematical satellite streaks around g_{200}-type matrix reflections.[2] Dislocation parameters are given in Table 2.8. Regardless of the metallurgical preconditions, no big difference can be observed among the specimens examined.

Table 2.6. Heat and mechanical treatment

	JPCA	J316
Solution annealed (SA)	1100°C × 1 h	1050°C × 0.5 h
Cold worked (CW)	20 and 20%	20%

J1352

(*a*)

J1420

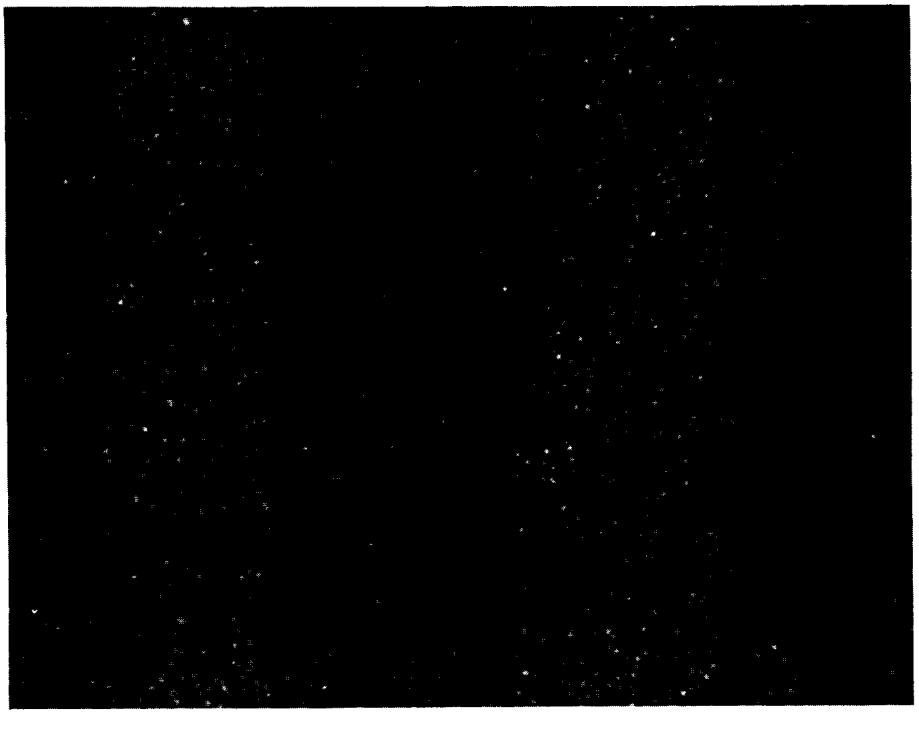

(*b*)

0.0250 μm

Fig. 2.11. Cavity microstructure of (*a*) JPCA-SA and (*b*) J316-SA after irradiation in HFIR to 30 dpa.

Table 2.7. Cavity data for JPCA and J316 stainless steels irradiated in HFIR

Specimen	Condition	Displacement damage (dpa)	Temperature (°C)	Helium content (at. ppm)	Type	Average diameter (nm)	Density (cavities/m^3)	Cavity volume fraction (%)	R[a]
JPCA	SA	34.0	300	2500	Bubble	2.9	1.9×10^{23}	0.23	0.6
	10% CW					3.0	2.1×10^{23}	0.31	0.8
	20% CW					2.6	2.3×10^{23}	0.21	0.5
J316	SA	33.0	300	2100	Bubble	2.7	3.0×10^{23}	0.29	0.8
	20% CW					2.5	3.5×10^{23}	0.28	0.7

[a]Ratio of calculated helium concentration for specimens from cavity microstructure to that calculated for transmutation.

Table 2.8. Dislocation parameters for JPCA and J316 stainless steels irradiated in HFIR

Specimen		Dislocation parameters	
		Average diameter (nm)	Number density (m^{-3})
JPCA	SA	11.5	1.2×10^{22}
JPCA	10% CW	10	1.6×10^{22}
JPCA	20% CW	10.6	2.5×10^{22}
J316	SA	10.3	1.3×10^{22}
	20% CW	10.4	1.5×10^{22}

Figure 2.12 shows the radiation-produced precipitation in 20% CW JPCA. The spacing of Moiré fringes of the particles is 1.0 nm, and the direction of the fringes is perpendicular to <200> reflections of the matrix, indicating that these particles are MC-type precipitates that have a cube-on-cube relationship with the matrix. Precipitation has not yet been observed in J316.

J1568

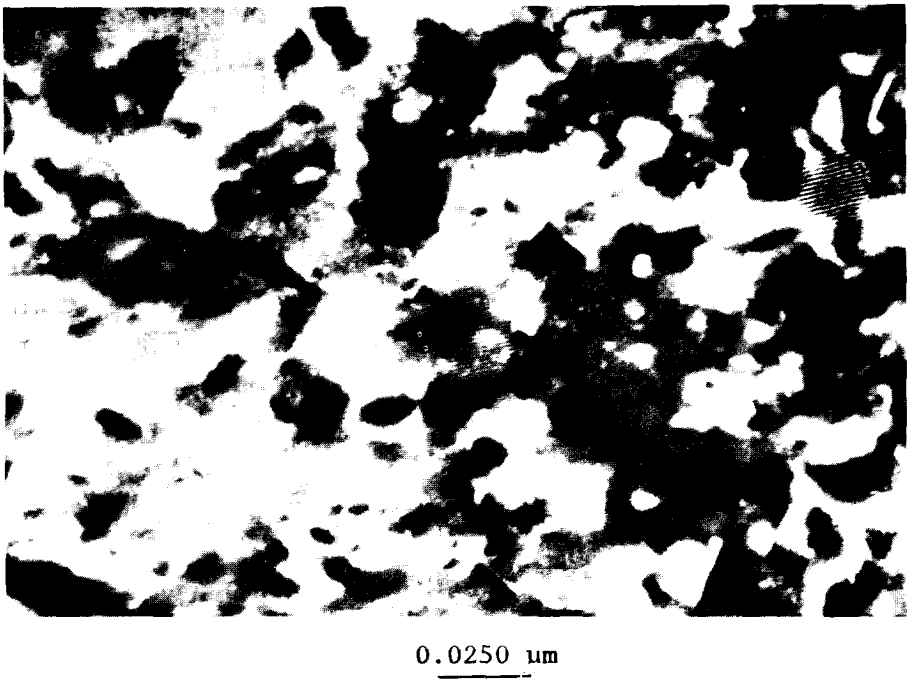

Fig. 2.12. Distribution of MC precipitates in JPCA-20% CW after irradiation in HFIR to 30 dpa at 300°C.

3. ORR SPECTRAL-TAILORING EXPERIMENTS

Spectral-tailoring experiments in the ORR are a part of the program of U.S.-Japan collaborative testing. The experimental technique was described in the last annual progress report.[1] Under the U.S.-Japan collaboration, two spectral-tailoring capsules are being irradiated. Capsule MFE–7J, which is irradiated at 330 and 400°C, is of a conventional design in which heat transfer is provided by a liquid-metal (NaK) medium. Capsule MFE-6J has an outer region in which the specimens are in contact with the ORR cooling water at 60°C. The inner 200°C region was especially challenging.

Since NaK does not wet stainless steel below 300°C, it would not be a good heat-transfer medium. The design approach selected was to use a solid piece of aluminum as the heat-transfer medium. Carefully machined slots in the aluminum were to contain flat tensile specimens; round holes provided containment for pressurized tubes and TEM disk packets. It was

also found convenient to put the 60°C region outside the 200°C zone instead of having one above the other. A schematic representation of MFE-6J is shown in Fig. 3.1.

3.1 EXPERIMENT OBJECTIVES

When the U.S.-Japan Collaborative Program using spectral-tailoring capsules was originally conceived (October 1981), the emphasis in the United States was focused on obtaining an engineering data base for the next-generation fusion reactor, especially the Engineering Power Reactor (EPR). Likewise in Japan, the focus was to obtain a data base for the structural alloy to be used in the Fusion Engineering Reactor (FER). Low-temperature capsule (60/200°C) experiments in the United States were especially important because higher temperature data (300/400/500/600°C) were already being obtained in the U.S. spectral-tailoring capsules MFE-4A and -4B. Thus, the original objectives were primarily focused on an engineering data base and on a direct comparison of U.S. and Japanese alloys under the same test conditions.

More recently (~1984) the focus of the U.S. fusion materials program has been redirected toward basic fusion materials research leading to the development of new materials with properties that enhance the economic and environmental potential of fusion. Low-activation alloys with good irradiation properties that are relatively easy to dispose of are especially attractive environmentally.

The U.S. test matrix for MFE-6J and -7J capsules contains specimens designed to accomplish both the original and new objectives. Engineering data are being obtained on type 316 stainless steel, U.S. PCA, and on HT-9. At the same time, data will be obtained on a variety of research and low-activation alloys at both ORNL and Hanford Engineering Development Laboratory (HEDL). Experiments with JAERI specimens are designed to accomplish both original and new objectives; however, priority will be given to the engineering data base for the FER. A comparison of results obtained with MFE-6J and -7J capsules with those of MFE-4A and -4B will provide the needed direct similarities and differences between U.S. and Japanese structural alloys.

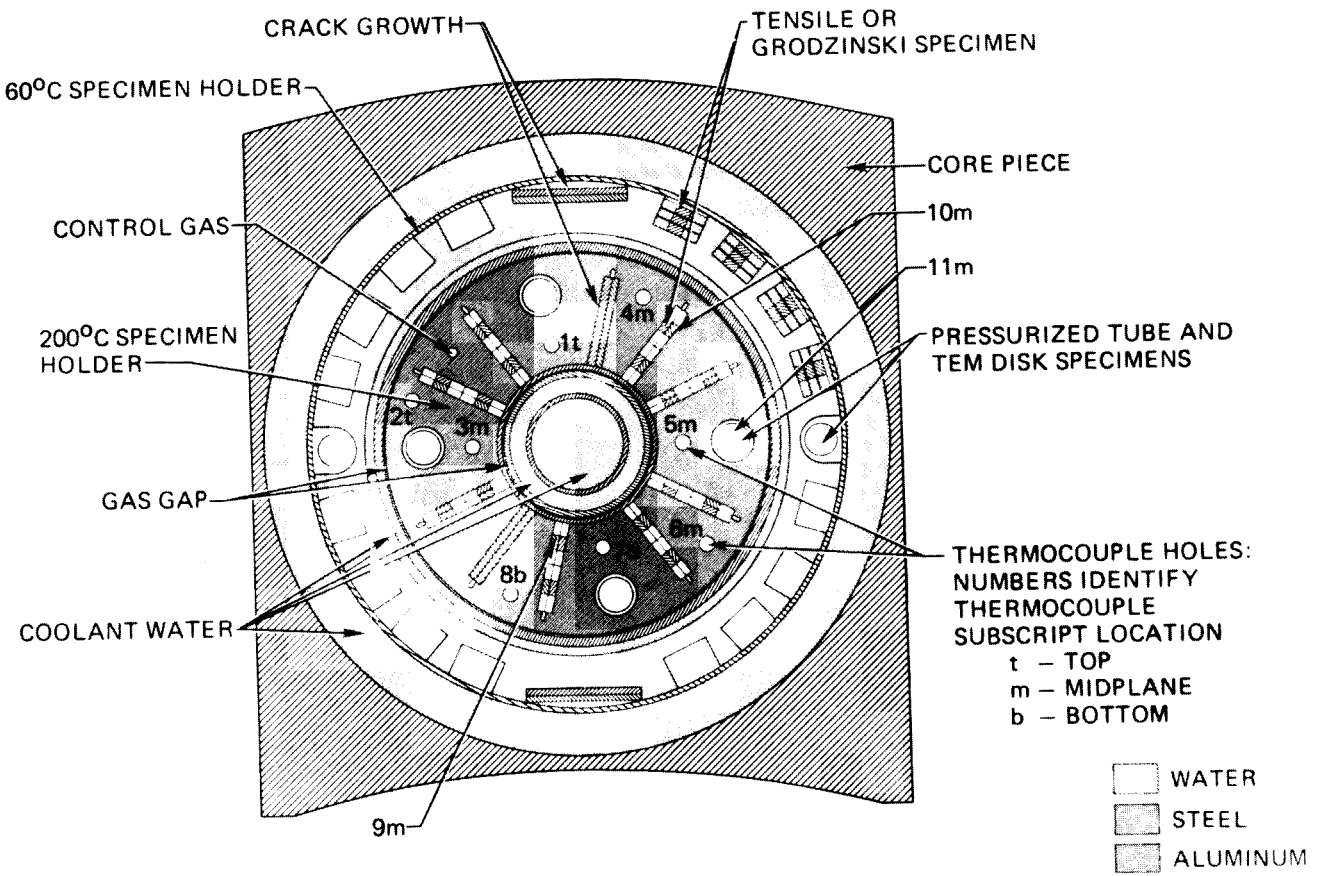

Fig. 3.1. Cross section of the MFE-6J capsule with typical test specimen locations.

The basic studies in the ORNL program are a collaborative effort among the ORNL Basic Energy Sciences (BES) Radiation Effects Program, Alloy Development for Irradiation Performance (ADIP), and Damage Analysis and Fundamental Studies (DAFS). As part of this collaboration, the programs have initiated an effort to prepare a combined experiment that would constitute a part of the U.S. side of the U.S.-Japan ORR test. The experiment consists of a joint effort with the fusion program on studies of irradiation creep and ceramics irradiation, together with other research on swelling, microstructural development, and mechanical properties.

3.1.1 Irradiation Creep

Irradiation creep behavior under neutron irradiation of materials of interest is relatively unknown at low temperatures, such as those available in this experiment. To our knowledge, there are no data at temperatures as low as 60 and 200°C. Furthermore, systematic data covering creep, swelling, and microstructure in high-purity simple alloys are also lacking. Such data are highly desirable in our theoretical efforts toward a quantitative understanding of mechanisms of irradiation creep and, in particular, the relationships of irradiation creep to swelling.

Four simple alloys in the form of pressurized tubes are used in the experiment. Also used are tubes of austenitic stainless steel PCA and ferritic stainless steel HT-9. Corresponding unstressed tubes and TEM specimen disks are used to provide baseline data on swelling and microstructure. The four simple alloys are the ferritic Fe-16Cr and the austenitics Fe-13Cr-15Ni, Fe-13Cr-35Ni, and Fe-13Cr-15Ni, with titanium and carbon added.

The ferritic alloy should be particularly interesting at the lower temperature, since materials of this type exhibit swelling and significant dislocation evolution at lower temperatures than austenitic alloys. A high-purity binary alloy was selected to study the irradiation response in an alloy with a simple preirradiation microstructure, thus facilitating interpretation of the experiment with modeling. The chromium content was dictated by the low-corrosion requirements for materials placed in the

cooling water of the ORR (60°C irradiation). A minimum level of 15% chromium was suggested to avoid any possible contamination of the reactor pool. The alloy was arc-melted from starting materials of MARZ-grade iron (99.99%$^{+}$) and 10CHROME chromium (99.996%$^{+}$). For a preliminary test heat fabricated in the same manner as the final alloy, metallic impurity concentrations were less than 5 wt ppm, and the total interstitial impurity concentration was about 100 wt ppm. Planned postirradiation analyses included correlation of the creep results with the microstructure.

The simple austenitic alloys were similarly selected to facilitate understanding of the creep-swelling interaction. Comparisons of the 15Ni ternary with the 35Ni ternary will provide information on relative creep rates in two alloys known to exhibit large differences in swelling and microstructure. In our previous work the 35Ni ternary proved highly resistant to swelling, whereas the 15Ni ternary swelled readily. The 15Ni ternary will also provide a good comparison with the creep and microstructural behavior of the ferritic alloy. The alloy containing titanium and carbon is expected to form a fine dispersion of TiC precipitates during irradiation. This is a microstructural feature that imparts swelling resistance, as our previous work has shown. Therefore, the creep response of this swelling-resistant alloy will be of great interest.

The alloys PCA and HT-9 were included to provide further detailed information on alloys of direct interest for fusion reactor application.

3.1.2 Embrittlement

Several experiments using SS-3 tensiles have been included to identify various mechanisms involved in grain boundary embrittlement. The first experiment addresses the effect of the segregation of Ti, Al, and Si and the precipitation of α' on grain boundary strength in both nickel and an Fe-15Cr-15Ni alloy. A second experiment explores the effects of helium on grain boundary strength in body-centered cubic (bcc) iron; doping with boron is used to generate helium. The third experiment explores the behavior of helium in zirconium, a material that is highly resistant to intergranular creep cavitation. SS-3 tensile specimens are also included for a set of both simple and more complex engineering alloys based on the

Fe-15Cr-15Ni system. The primary objective of these experiments is to investigate radiation hardening in a set of well-characterized alloys for which extensive swelling and microstructural data already exist.

3.1.3 Microstructures

Microstructural information from the previously described specimens will be obtained by analytical electron microscopy. Additional specimens are included in the form of TEM disks that consist of specimens based on the B–series and E–series austenitics (previously described) and a series of high-purity Fe–C and Fe-Cr-C alloys. The austenitics are used to study phase stability and its interactions with swelling and mechanical property changes. In particular, the association of cavities with precipitates and the effects of the precipitate interfacial area on swelling in precipitates (such as TiC and Fe_2P) are of great interest in controlling swelling. Ferritic specimens were included to study the effects of carbon on swelling and dislocation evolution. The dislocation structures are particularly interesting in ferritic materials. Interstitial dislocation loops with $\underline{b}$ = a<l00> are often observed in irradiated ferritic materials, whereas loops in other bcc materials have $\underline{b}$ = a/2<111>. The effect of the a<l00> loops on the nucleation and growth of cavities is not known. The dose to the onset of swelling in ferritic materials is relatively large and may result, in part, from the unusual dislocation evolution. Impurity segregation at the dislocation loops and cavities may also influence the damage evolution. Carbon, in particular, is known to segregate to {100} planes, as evidenced by observing the effects of carbides on these planes. In this experiment, the effects of both interstitial carbon and carbide precipitates will be determined. The alloys with the higher carbon concentrations approach the carbon levels contained in ferritic steels and contain precipitates; the alloys with low-carbon concentrations contain no precipitates. The relatively low irradiation temperatures (200, 300, and 400°C) complement those in a similar experiment conducted in the Fast-Flux Test Facility (FFTF). In the FFTF experiment, the same alloys were irradiated at temperatures of 470 to 585°C. Although the FFTF experiment was conducted primarily to study high-temperature structures

and the swelling variation, the lower temperatures in the ORR should permit comparisons of dislocation loop structures and early stages of cavity nucleation.

3.1.4 Ceramics

Ceramics have been proposed for a variety of fusion applications; however, little irradiation data exists on most ceramics at the fluences and temperatures of interest. Since the spectral-tailoring capsules offer the range of fluences (up to 30 dpa) and temperatures (60-400°C) of greatest interest, it was decided to include selected ceramic materials in the form of TEM disks in capsules MFE-6J and -7J. The compositions, forms, and investigators are listed in Table 3.1. Ceramics 1 through 3 and 6 through 7 (Table 3.1) are compositions and forms of direct relevance to fusion application. Ceramics 4 and 5 will provide additional information about the effects of helium on swelling. Helium is produced either by lithium fissions (composition 4) or by the two-step neutron-^{58}Ni reaction that produces ^{56}Fe and helium (composition 5). Examination by TEM after irradiation will provide important data on swelling and microstructural changes, and microhardness testing will provide information about irradiation-induced changes in the fracture toughness.

Table 3.1. Ceramics being irradiated in capsules MFE-6J and –7J

Number	Composition	Form	Investigator
1	Si_3N_4	Polycrystalline	F. W. Clinard, Jr.
2	$MgAlO_z$	Polycrystalline	F. W. Clinard, Jr.
3	$MgAlO_z$	Single crystal	F. W. Clinard, Jr.
4	MgO + 0.1Li	Single crystal	L. L. Horton
5	MgO + 0.1Ni	Single crystal	L. L. Horton
6	MgO	Single crystal	L. L. Horton
7	Al_2O_3	Single crystal	P. F. Becher

3.1.5 Objective of the HEDL Test Matrix

The HEDL test matrix consists of crack-growth specimens, SS-3 tensile specimens of experimental ferritic alloys, and TEM disks of simple Fe-Ni-Cr and Fe-Cr-Mn ternaries, together with solute modifications to

these ternaries. The crack-growth specimens consist of 20%-CW type 316 stainless steel (X-15893) and 25%-CW PCA (K-280). Since these alloys were irradiated in capsules MFE-4A and -4B, the data can now be expanded over a wider temperature range. The matrix of tensile specimens consists of a series of low-activation ferritic alloys with chromium contents between 2.25% and 12%, with V, W, and Mn as alloying additions. These specimens will provide information on irradiation embrittlement of low-activation alloys. The TEM disk arrays are designed to explore the swelling behavior of high-purity Fe-Ni-Cr and Fe-Cr-Mn alloys with and without low-activation solute additions. The specimens will also provide information on the fundamental mechanisms of swelling and the effects of helium.

3.1.6 Objectives of the JAERI Program

The primary objective of the Japan Atomic Energy Research Institute (JAERI) part of the ORR spectral-tailoring capsule is to obtain engineering data on candidate structural materials for the next fusion reactor in Japan. Major emphasis is placed on the understanding of the irradiation response of type 316 stainless steel and the Japanese prime candidate alloy (JPCA) with respect to swelling, irradiation creep, tensile properties, and fracture behavior. It is expected that JPCA will show more improved resistance to swelling and helium embrittlement at an elevated temperature than does type 316 stainless steel. To further enhance its behavior, JPCA is being tested in the 15% to 20% cold-worked condition and/or is being heat treated to control solutes and precipitate distributions. Solution-annealed JPCA is also being tested. Since welding is required for blanket assembly, welded joints made by the tungsten inert gas (TIG) method are a part of the JAERI test matrix.

A second objective of the JAERI test program in the ORR is to conduct fundamental studies leading to a further understanding of radiation-induced segregation, swelling, embrittlement, and resistance to stress corrosion cracking. Not only the austenitic stainless steels, but also ferritic and dual-phase alloys are included. Alloys designated C and K are compositional modifications to JPCA, with improved resistance to stress corrosion cracking in water (a possible coolant for next-generation

fusion reactors). The C and K alloys have lower carbon contents and small amounts of titanium and/or niobium to compensate for strength reduction. The nickel and chromium contents are also adjusted to maintain phase stability. In the case of ferritic steels, 9Cr–2Mo alloys are being compared with HT-9. One all-martensitic alloy is included to determine the effects of vanadium and tungsten on HT-9.

The fundamental studies include a series of dual-phase alloys. Since austenitic alloys suffer helium embrittlement and ferritic alloys show a ductile-to-brittle transition, an alloy resistant to both phenomena is being sought. Dual–phase alloys may offer this possibility. Strain-aged and recrystallized (SAR) austenitic steels are also possibly resistant to helium embrittlement; these alloys are 50% cold worked and then aged at 650°C for 15 h and at 775°C for 5 h. This treatment reduces the grain size to ASTM 10-11 and provides many grain boundaries to trap helium. A pure Fe-Ni-Cr ternary is being irradiated to determine the swelling behavior of simple ternaries; low-activation manganese steels and Incoloy 800 (a good breeder reactor alloy) are also being evaluated.

Because of the limited availability of space, fundamental studies are limited to TEM disks, and microstructural analysis will be the primary evaluation technique.

3.2 TEST MATRIX

The test matrix for the MFE-6J and -7J capsules is shown in Table 3.2. The types of specimens and the source of each are indicated together with the number to be removed for testing at the 10-, 20-, and 30-dpa levels at each temperature. The compositions of the alloys are given in Tables 3.3 through 3.5. Specimen descriptions and loading lists are given in the following sections.

3.3 PRESSURIZED TUBES

Irradiation creep is being investigated through the use of pressurized-tube specimens. This technique, which was used in the earlier spectral-tailoring capsules MFE-4A and -B,[3] has proven successful at ORNL,[4] HEDL,[5] and at KRZ Karlsruhe.[6] The design of the pressurized tube is shown in

Table 3.2. Test matrix for the MFE-6J and -7J capsules

Type	Source	Number of specimens[a]											
		60			200			330			400		
		10	20	30	10	20	30	10	20	30	10	20	30
Pressurized tubes	ORNL	32	32	32	16	16	16	39	39	39	33	33	33
	JAERI	6	6	6	10	10	10	6	6	6	6	6	6
Tube blanks	ORNL	6	6	6	6	6	6	6	6	6	6	6	6
	JAERI	3	3	3	3	3	3	3	3	3	3	3	3
TEM disks	ORNL	2	1	1	2	1	1	6	1	1	7	1	1
	HEDL	0	0	0	0	0	0	2	1	1	2	1	1
	JAERI	3	0	2	5	0	2	4	0	2	4	0	2
SS1 tensiles	ORNL	9	0	20	10	0	24	11	0	0	13	0	0
	JAERI	40	18	12	35	12	12	46	12	18	40	12	12
SS3 tensiles	ORNL	7	8	28	8	8	28	16	0	0	22	0	0
	HEDL	17	8	10	17	8	10	15	7	8	15	7	8
Grodzinski fatigue	JAERI	24	16	16	8	8	8	24	16	16	24	8	8
Crack growth	JAERI	18	0	0	18	0	0	10	0	0	10	0	0
	HEDL	6	6	6	6	6	6	0	0	0	0	0	0
Rod tensiles	JAERI	0	0	0	0	0	0	2	0	2	0	0	0
HFIR fatigue	JAERI	0	0	0	0	0	0	0	0	0	3	0	2

[a]Irradiated to 10, 20, and 30 dpa.

Fig. 3.2. After fabrication, the tube is placed in a pressure chamber that has a glass window. The chamber is pressurized with helium gas, and the pinhole in the end cap is laser welded shut. Weld parameters are chosen to give a full–penetration weld. The Japanese tubes in MFE–6J and -7J were fabricated at HEDL and have a different end cap weld.

To obtain irradiation creep data, the pressurized tubes are periodically removed from the reactor, and the diameter profiles are measured. The average diameter of the central three-fifths of each tube is used in the creep analysis. A correction for swelling is made based on density measurements of 6.35-mm-long tube specimens prepared with no end caps.

Table 3.3. Alloys in the ORNL test matrix for the MFE-6J and -7J capsules

Alloy	Composition, wt %																						
	Li	B	C	N	O	Al	Si	P	S	Ti	V	Cr	Mn	Fe	Co	Ni	Cu	Zr	Nb	Mo	Sn	Ta	W
316 SS	--	0.0004	0.061	--	--	--	0.67	0.037	0.02	--	--	17.3	1.7	bal	0.3	12.4	0.3	--	--	2.1	--	--	--
PCA	--	0.0005	0.047	0.009	--	0.03	0.42	0.009	0.003	0.24	0.02	14.0	1.8	bal	--	16.2	0.05	--	0.02	2.3	--	0.001	--
HT-9	--	--	0.2	0.027	--	0.006	0.17	0.016	0.003	0.001	0.28	12.1	0.57	bal	--	0.51	--	--	--	1.04	--	--	0.45
1B	--	--	0.008	0.012	--	--	0.04	0.003	--	--	--	13.5	--	bal	--	15.0	--	--	--	--	--	--	--
2B	--	--	0.008	0.012	--	--	0.04	0.003	0.007	--	--	13.5	--	bal	--	35.0	--	--	--	--	--	--	--
3B	--	--	0.04	--	--	--	0.04	0.003	0.25	0.25	--	13.5	--	bal	--	15.0	--	--	--	0.01	--	--	--
5A	--	--	--	--	--	--	--	--	--	--	--	16.0	--	bal	--	--	--	--	--	--	--	--	--
B1	--	--	0.006	0.010	0.03	--	0.04	0.003	0.007	--	--	13.8	--	bal	--	15.0	--	--	--	0.01	--	--	--
B2	--	--	0.008	0.011	0.01	--	0.04	0.004	0.007	0.17	--	13.7	--	bal	--	15.0	--	--	--	0.01	--	--	--
B3	--	--	0.009	0.009	0.02	--	0.83	0.003	0.007	--	--	13.7	--	bal	--	15.0	--	--	--	0.01	--	--	--
B5	--	--	0.04	0.011	0.004	--	0.04	0.003	0.007	0.17	--	13.7	--	bal	--	14.9	--	--	--	0.01	--	--	--
B6	--	--	0.05	0.011	0.003	--	0.01	0.003	0.007	0.16	--	13.4	--	bal	--	15.0	--	--	--	1.97	--	--	--
B7	--	--	0.04	0.011	0.004	--	0.83	0.003	0.007	0.10	--	13.6	--	bal	--	15.0	--	--	--	0.01	--	--	--
B9	--	--	0.005	0.009	0.03	--	0.04	0.049	0.007	--	--	13.7	--	bal	--	15.2	--	--	--	0.01	--	--	--
B10	--	--	0.007	0.009	0.020	--	0.84	0.05	0.007	--	--	13.6	--	bal	--	15.2	--	--	--	0.01	--	--	--
B11	--	--	0.041	0.011	0.013	--	0.04	0.049	0.007	0.18	--	13.6	--	bal	--	15.2	--	--	--	0.01	--	--	--
B12	--	--	0.044	0.010	0.004	--	0.83	0.049	0.007	0.17	--	13.6	--	bal	--	15.2	--	--	--	0.01	--	--	--
B13	--	--	0.025	0.007	0.005	--	0.04	0.003	0.007	--	--	13.4	--	bal	--	14.9	--	--	0.40	0.01	--	--	--
E1	--	0.001	0.06	0.010	0.004	--	0.82	0.002	0.007	0.19	--	13.1	2.1	bal	--	15.1	--	--	0.01	1.98	--	--	--
E2	--	--	0.055	0.011	0.003	--	0.80	0.003	0.007	0.19	--	13.4	2.2	bal	--	15.0	--	--	--	0.01	--	--	--
E3	--	--	0.053	0.011	0.004	--	0.82	0.003	0.007	0.17	--	13.2	--	bal	--	15.1	--	--	--	1.97	--	--	--
E4	--	--	0.040	0.008	0.006	--	0.83	0.003	0.007	--	--	13.2	2.1	bal	--	15.1	--	--	--	1.98	--	--	--
E5	--	--	0.009	0.010	0.008	--	0.83	0.002	0.007	0.17	--	13.2	2.1	bal	--	15.1	--	--	--	1.98	--	--	--
E6	--	--	0.047	0.010	0.003	--	0.37	0.002	0.007	0.17	--	13.2	2.1	bal	--	15.1	--	--	0.01	1.97	--	--	--
E8	--	--	0.054	0.011	0.004	--	0.84	0.044	0.007	0.17	--	13.1	2.1	bal	--	15.1	--	--	0.01	1.98	--	--	--
E9	--	--	0.036	0.010	0.003	--	0.35	0.043	0.007	0.17	--	13.2	2.1	bal	--	15.1	--	--	--	1.97	--	--	--
E10	--	0.001	0.046	0.010	0.004	--	--	0.046	0.007	0.18	--	13.3	2.1	bal	--	15.1	--	--	0.01	1.98	--	--	--
E11	--	--	0.035	0.007	0.003	--	0.84	0.002	0.007	--	--	13.2	2.1	bal	--	15.2	--	--	0.45	1.99	--	--	--
E12	--	0.002	0.023	0.007	0.005	--	0.35	0.003	0.007	--	--	13.2	2.1	bal	--	15.1	--	--	0.42	1.95	--	--	--
E13	--	--	0.019	0.008	0.009	--	0.01	0.002	0.007	--	--	13.2	2.1	bal	--	15.1	--	--	0.41	1.95	--	--	--
E14	--	--	0.044	0.010	0.003	--	0.01	0.002	0.007	0.09	--	13.2	2.1	bal	--	15.1	--	--	0.23	1.97	--	--	--
M1	--	--	--	--	--	--	--	--	--	--	--	7.0	--	bal	--	15.0	--	--	--	--	--	--	--
M3	--	--	--	--	--	--	--	--	--	--	--	7.0	--	bal	--	35.0	--	--	--	--	--	--	--
M4	--	--	--	--	--	--	--	--	--	--	--	7.0	--	--	--	45.0	--	--	--	--	--	--	--
M6	--	--	--	--	--	--	--	--	--	--	--	15.0	--	--	--	45.0	--	--	--	--	--	--	--
M9	--	--	--	--	--	--	--	--	--	--	--	2.0	--	--	--	35.0	--	--	--	--	--	--	--
M11	--	--	--	--	--	--	--	--	--	--	--	--	--	bal	--	35.0	--	--	--	--	--	--	--

Table 3.3. (continued)

Alloy	Composition, wt %																						
	Li	B	C	N	O	Al	Si	P	S	Ti	V	Cr	Mn	Fe	Co	Ni	Cu	Zr	Nb	Mo	Sn	Ta	W
C	--	--	0.01	--	--	--	--	--	--	--	--	--	--	bal	--	--	--	--	--	--	--	--	--
D	--	--	0.02	--	--	--	--	--	--	--	--	--	--	bal	--	--	--	--	--	--	--	--	--
E	--	--	0.04	--	--	--	--	--	--	--	--	--	--	bal	--	--	--	--	--	--	--	--	--
H	--	--	0.10	--	--	--	--	--	--	--	--	--	--	bal	--	--	--	--	--	--	--	--	--
K	--	--	0.15	--	--	--	--	--	--	--	--	--	--	bal	--	--	--	--	--	--	--	--	--
L	--	--	0.20	--	--	--	--	--	--	--	--	--	--	bal	--	--	--	--	--	--	--	--	--
M	--	--	--	--	--	--	--	--	--	--	--	12.0	--	bal	--	--	--	--	--	--	--	--	--
P	--	--	0.12	--	--	--	--	--	--	--	--	12.0	--	bal	--	--	--	--	--	--	--	--	--
Zr1	--	0.1E-4	0.008	0.004	0.14	--	--	--	--	--	--	--	--	--	--	--	--	bal	--	--	--	--	--
ZrB1	--	4.4E-4[a]	--	--	--	--	--	--	--	--	--	--	--	--	--	--	--	bal	--	--	--	--	--
ZrB2	--	0.22E-4[a]	--	--	--	--	--	--	--	--	--	--	--	--	--	--	--	bal	--	--	--	--	--
Zr4	--	--	--	--	--	--	--	--	--	--	--	0.094	--	0.20	--	--	--	bal	--	--	1.51	--	--
Zr4-Li3	26E-4	--	--	--	--	--	--	--	--	--	--	0.10	--	0.20	--	--	--	bal	--	--	1.52	--	--
Ni-1Si	--	--	--	--	--	--	0.48	--	--	--	--	--	--	--	--	bal	--	--	--	--	--	--	--
Ni-1Ti	--	--	--	--	--	--	--	--	--	0.82	--	--	--	--	--	bal	--	--	--	--	--	--	--
Ni-1Al	--	--	--	--	--	0.46	--	--	--	--	--	--	--	--	--	bal	--	--	--	--	--	--	--
Ni-8Si	--	--	--	--	--	--	4.0	--	--	--	--	--	--	--	--	bal	--	--	--	--	--	--	--
Fe-Ni-Cr	--	--	0.006	--	--	--	0.04	--	--	--	--	13.8	--	bal	--	14.9	--	--	--	--	--	--	--
Fe-Ni-Cr-Li2	9.4E-4	--	0.006	--	--	--	0.04	--	--	--	--	13.8	--	bal	--	14.9	--	--	--	--	--	--	--
Fe-Ni-Cr(1Si)	--	--	--	--	--	--	0.52	--	--	--	--	13.7	--	bal	--	14.6	--	--	--	--	--	--	--
Fe-Ni-Cr(1Ti)	--	--	--	--	--	--	0.04	--	--	0.82	--	13.7	--	bal	--	14.8	--	--	--	--	--	--	--
Fe-Ni-Cr(1Al)	--	--	--	--	--	0.46	0.04	--	--	--	--	13.7	--	bal	--	14.8	--	--	--	--	--	--	--
Fe	--	--	--	--	--	--	--	--	--	--	--	--	--	bal	--	--	--	--	--	--	--	--	--
Fe-Li3	8E-4	--	--	--	--	--	--	--	--	--	--	--	--	bal	--	--	--	--	--	--	--	--	--
Fe-lowB	--	10E-4[a]	--	--	--	--	--	--	--	--	--	--	--	bal	--	--	--	--	--	--	--	--	--
Fe-highB	--	0.010	--	--	--	--	--	--	--	--	--	--	--	bal	--	--	--	--	--	--	--	--	--
PCA-20	--	0.001	0.083	0.006	--	--	0.42	0.068	0.007	0.25	0.51	13.83	2.06	bal	0.01	16.12	0.01	--	0.10	2.48	--	--	--
PCMA-6	--	--	0.18	0.003	--	--	0.01	--	--	--	--	15.94	14.59	bal	--	0.01	0.03	--	--	0.01	--	--	--

[a] ^{10}B.

Table 3.4. Alloys in the HEDL test matrix for the MFE-6J and -7J capsules

Alloy	Composition, wt %																	
	B	C	N	Al	Si	P	S	Ti	V	Cr	Mn	Fe	Ni	Cu	Nb	Mo	Ta	W
Low-Activation																		
VO-2262	—	0.086	—	—	0.08	—	0.003	—	0.50	2.32	—	bal	0.02	—	—	—	—	—
VO-2263	—	0.093	—	—	0.08	—	0.002	—	1.01	2.38	—	bal	0.01	—	—	—	—	—
VO-2264	—	0.096	—	—	0.09	—	0.003	—	0.52	9.13	0.02	bal	—	—	—	—	—	0.01
VO-2265	—	0.197	—	—	0.09	—	0.003	—	1.23	9.14	1.08	bal	—	—	—	—	—	0.02
VO-2266	—	0.097	—	—	0.09	—	0.003	—	0.51	9.02	2.68	bal	—	—	—	—	—	0.01
VO-2267	—	0.089	—	—	0.10	—	0.005	—	1.05	12.2	6.47	bal	0.01	—	—	—	—	—
VO-2268	—	0.101	—	—	0.10	—	0.004	—	0.27	8.82	2.44	bal	—	—	—	—	—	0.89
VO-2269	—	0.097	—	—	0.11	—	0.004	—	0.28	11.8	6.47	bal	—	—	—	—	—	0.89
UC-19	—	0.11	—	0.043	0.30	0.007	0.015	0.043	1.50	2.46	0.30	bal	0.05	0.04	—	0.02	—	—
GA-3X	—	0.15	—	—	—	—	—	—	0.30	9.0	—	bal	—	—	—	—	—	2.5
VO-2702	—	0.093	—	—	0.10	—	0.004	—	0.23	12.0	6.56	bal	—	—	—	—	0.14	0.82
VO-2700	—	0.111	—	—	0.11	—	0.005	—	1.00	12.0	6.50	bal	0.02	—	0.02	—	—	—
VO-2754	—	0.1	—	—	—	—	—	—	0.3	12.0	6.5	bal	—	—	—	—	0.2	1.0
VO-2755	—	0.1	—	—	—	—	—	—	1.0	12.0	8.0	bal	—	—	—	—	0.2	0.2
10996	—	0.10	—	—	0.12	0.007	0.005	—	0.21	11.8	3.33	bal	0.01	—	—	—	—	—
10998	—	0.11	—	—	0.10	0.007	0.006	—	0.10	12.0	6.57	bal	—	—	—	—	—	—
Special Alloys																		
E18	—	—	—	—	—	—	—	—	—	15	—	bal	12.0	—	—	—	—	—
E90	—	—	—	—	—	—	—	—	—	15.0	—	bal	15.0	—	—	—	—	—
E19	—	—	—	—	—	—	—	—	—	15.0	—	bal	20.0	—	—	—	—	—
E20	—	—	—	—	—	—	—	—	—	15.0	—	bal	25.0	—	—	—	—	—
E22	—	—	—	—	—	—	—	—	—	15.0	—	bal	35.0	—	—	—	—	—
E23	—	—	—	—	—	—	—	—	—	15.0	—	bal	45.0	—	—	—	—	—
R58	—	—	—	—	—	—	—	—	—	15.0	—	bal	45.0	—	—	—	—	—
E37	—	—	—	—	—	—	—	—	—	8.0	—	bal	35.0	—	—	—	—	—
GE5	—	—	—	—	—	—	—	—	—	—	—	bal	35.0	—	—	—	—	—
GE10	—	—	—	—	—	—	—	—	—	—	—	bal	45.0	—	—	—	—	—
GE26	—	—	—	—	—	—	—	—	—	—	—	bal	60.0	—	—	—	—	—
GE29	—	—	—	—	—	—	—	—	—	—	—	bal	75.0	—	—	—	—	—
E38	—	—	—	—	—	—	—	—	—	20.0	—	bal	35.0	—	—	—	—	—
R61	—	—	—	—	—	—	—	—	—	5.0	—	bal	45.0	—	—	—	—	—
R48	—	—	—	—	—	—	—	—	—	10.0	—	bal	45.0	—	—	—	—	—
R72	—	—	—	—	—	—	—	—	—	—	30.0	bal	—	—	—	—	—	—
R73	—	—	—	—	—	—	—	—	—	5.0	30.0	bal	—	—	—	—	—	—
R74	—	—	—	—	—	—	—	—	—	10.0	30.0	bal	—	—	—	—	—	—
R76	0.005	0.60	0.05	—	0.4	0.05	—	—	—	2.0	30.0	bal	0.5	—	—	—	—	—
R66	—	—	—	—	—	—	—	—	—	5.0	15.0	bal	—	—	—	—	—	—
R83	0.005	0.60	0.05	—	1.0	0.05	—	—	—	5.0	15.0	bal	0.5	—	—	—	—	—
R67	—	—	—	—	—	—	—	—	—	15.0	15.0	bal	—	—	—	—	—	—
R87	0.005	0.10	0.10	—	1.0	0.05	—	—	—	15.0	15.0	bal	0.5	—	—	—	—	—
R69	—	—	—	—	—	—	—	—	—	10.0	20.0	bal	—	—	—	—	—	—
R70	—	—	—	—	—	—	—	—	—	15.0	20.0	bal	—	—	—	—	—	—
R71	—	—	—	—	—	—	—	—	—	—	25.0	bal	—	—	—	—	—	—
R75	—	—	—	—	—	—	—	—	—	—	35.0	bal	—	—	—	—	—	—

Table 3.5. Alloys in the JAERI test matrix for the MFE-6J and -7J capsules

Alloy	Composition, wt %																	
	C	N	O	Al	Si	P	S	Ti	V	Cr	Mn	Fe	Co	Ni	Cu	Nb	Mo	W
JPCA	0.05	0.0039	--	--	0.50	0.027	0.005	0.24	--	14.2	1.77	bal	0.002	15.6	--	--	2.28	--
C	0.02	0.0018	--	--	0.51	0.017	0.007	0.25	--	15.4	1.56	bal	--	15.6	--	0.08	2.4	--
K	0.02	0.004	--	--	0.48	0.015	0.005	0.29	--	18.0	1.46	bal	--	17.6	--	--	2.6	--
316	0.058	--	--	--	0.61	0.028	0.003	0.005	--	16.7	1.80	bal	--	13.5	--	--	2.46	--
HighNi																		
alloy I	0.06	--	--	--	0.31	--	--	0.23	--	12.9	1.78	bal	--	24.9	--	0.03	5.43	--
Q	0.007	--	--	--	0.16	0.003	0.003	0.01	--	13.0	1.50	bal	--	20.0	--	--	4.94	4.94
Ferritic steel	0.056	0.0069	--	0.04	0.74	0.008	0.0059	--	0.11	8.9	0.70	bal	--	1.37	0.02	0.06	2.46	0.01
HT-9	0.198	0.0104	--	--	0.32	0.009	0.0013	--	0.22	11.7	0.55	bal	0.01	0.65	--	--	1.05	0.44
Dual phase A	0.004	0.004	--	0.022	0.13	--	0.005	--	--	23.2	--	bal	0.01	17.9	--	--	--	--
B	0.005	0.007	--	0.016	0.13	--	0.005	--	--	23.2	--	bal	0.01	16.0	--	--	--	--
C	0.004	0.003	--	0.006	0.16	--	0.005	--	--	23.1	0.05	bal	0.01	15.0	--	--	--	--
D	0.003	0.006	--	0.004	0.17	--	0.005	--	--	22.9	0.11	bal	0.01	11.9	--	--	--	--
E	0.002	0.003	--	0.005	0.17	--	0.005	--	--	23.0	0.05	bal	0.01	8.31	--	--	--	--
K	0.012	0.024	--	0.004	0.18	--	0.004	--	--	23.1	0.17	bal	0.01	9.62	--	--	--	--
G	0.004	0.004	--	0.005	0.15	--	0.006	--	--	23.1	0.06	bal	0.01	16.0	--	--	--	--
I	0.004	0.003	--	0.005	0.18	--	0.005	--	--	23.2	0.04	bal	0.01	15.2	--	--	--	--
J	0.004	0.006	--	0.007	0.16	--	0.005	--	--	23.2	0.03	bal	0.01	15.3	--	--	--	--
SAR type 304	0.06	--	--	--	0.25	0.034	0.023	--	--	18.2	0.75	bal	--	8.1	--	--	0.13	--
SAR type 316	0.06	--	--	--	0.39	0.032	0.012	--	--	16.1	0.84	bal	--	10.0	--	--	2.01	--
SN-1	0.01	--	--	--	1.22	0.023	0.005	--	--	16.9	0.94	bal	--	13.9	0.07	--	0.09	--
SN-5	0.013	0.01	--	--	0.58	0.028	0.001	--	--	16.7	1.15	bal	--	8.49	--	--	--	--
HiMn steel 1	0.006	0.30	0.013	--	0.50	0.003	0.004	--	--	18.0	17.2	bal	--	0.01	--	--	0.01	--
HiMn steel 2	0.007	0.32	0.021	--	0.48	0.003	0.002	--	--	18.0	16.8	bal	--	2.01	--	--	0.01	--
All-Martensite	0.007	0.030	--	--	--	--	0.004	--	0.13	8.4	0.83	bal	--	--	0.29	0.055	1.79	--
Incoloy 800	0.02	--	--	--	0.4	--	0.002	0.56	--	20.8	0.9	bal	--	33.3	--	--	--	--
Pure SS																		
HP 12 Ni	0.005	0.02	--	--	0.005	--	--	--	--	17.1	--	bal	--	11.8	--	--	--	--
HP 35 Ni	0.003	0.01	--	--	0.006	--	--	--	--	17.1	--	bal	--	35.3	--	--	--	--
HP 50 Ni	0.003	0.007	--	--	0.007	--	--	--	--	17.1	--	bal	--	49.9	--	--	--	--

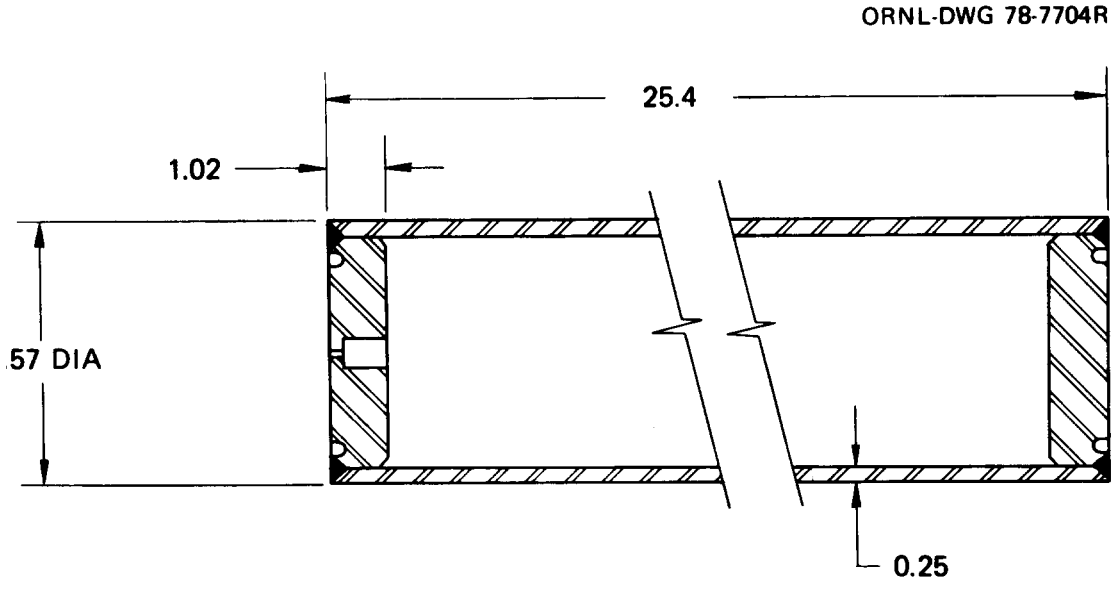

Fig. 3.2. Pressurized tube design; all dimensions are in millimeters.

Since the tubes are pressurized at a series of different pressures, the effect of stress at constant fluence can be determined for each alloy. The fluence dependence can be determined through the periodic examination of all tubes. The test matrix and hoop stresses for each tube are presented in Table 3.6.

3.4 TENSILE SPECIMENS

The tensile test matrix for capsules MFE–6J and -7J consists of SS–1–type specimens from ORNL and JAERI, SS-3-type specimens from ORNL and HEDL, and a few so-called submini specimens (normally used in HFIR) from JAERI. Specimen dimensions are shown in Figs. 3.3 through 3.5. The test matrix is presented in Tables 3.7 through 3.10.

3.5 FATIGUE SPECIMENS

Fatigue specimens (provided by JAERI) are of two types: Grodzinski sheet specimens and HFIR-type hourglass specimens. Sheet specimens (Fig. 3.6) can be used for tensile-tensile fatigue or bend testing; hourglass specimens (Fig. 3.7) are tested in the full tension-compression mode. The fatigue test matrix is given in Table 3.11.

Table 3.6. Test matrix for pressurized tubes in MFE-6J and -7J capsules

Alloy	Condition	Source	60°C		200°C		330°C		400°C	
			Identi-fication	Stress (MPa)	Identi-fication	Stress (MPa)	Identi-fication	Stress (MPa)	Identi-fication	Stress (MPa)
PCA	20% CW	ORNL	FA-1	0	FA-2	0	FA-1	0	FA-2	0
PCA	20% CW	ORNL	FA-51	50	FA-59	50	FA-33	50	FA-01	50
PCA	20% CW	ORNL	FA-36	100	FA-48	100	FA-19	100	FA-32	100
PCA	20% CW	ORNL	FA-53	150	FA-62	200	FA-27	200	FA-10	200
PCA	20% CW	ORNL	FA-58	200	-----	---	FA-34	200	FA-05	300
PCA	20% CW	ORNL	FA-24	200	-----	---	FA-08	300	FA-12	400
PCA	20% CW	ORNL	----	---	-----	---	FA-28	400	-----	---
HT-9	a	ORNL	SA28-1	0	SA28-2	0	SA-1	0	SA-2	0
HT-9	a	ORNL	SA-54	100	SA-21	200	SA-09	50	SA-58	50
HT-9	a	ORNL	SA-49	200	SA-30	400	SA-56	100	SA-37	100
HT-9	a	ORNL	SA-17	200	----	---	SA-05	200	SA-32	200
HT-9	a	ORNL	SA-41	280	----	---	SA-16	200	SA-53	300
HT-9	a	ORNL	SA-55	280	----	---	SA-01	300	SA-03	400
HT-9	a	ORNL	SA-24	300	----	---	SA-33	300	SA-31	400
			-----	---	----	---	SA-38	400	-----	---
1B	SA	ORNL	CA-1	0	CA-2	0	CA-1	0	CA-2	0
1B	SA	ORNL	C3-A4	5	C1-A6	5	C1-A0	5	C5-A2	5
1B	SA	ORNL	C1-A3	10	C2-A6	10	C4-A1	10	C3-A6	10
1B	SA	ORNL	C3-A0	30	C4-A9	30	C3-A1	20	C4-A2	20
1B	SA	ORNL	C3-A5	30	-----	---	C1-A9	27	C2-A4	30
1B	SA	ORNL	C3-A9	60	-----	---	C4-A6	30	C3-A2	40
1B	SA	ORNL	----	---	-----	---	C4-A3	40	C1-A1	40
2B	SA	ORNL	CB-1	0	CB-2	0	CB-1	0	CB-2	0
2B	SA	ORNL	C2-B8	5	C3-B2	5	C5-B3	5	C4-B4	5
2B	SA	ORNL	C2-B6	10	C1-B3	10	C4-B9	10	C3-B4	10
2B	SA	ORNL	C2-B5	30	C3-B1	30	C4-B5	20	C4-B2	20
2B	SA	ORNL	C2-B9	30	----	---	C3-B3	20	C4-B0	30
2B	SA	ORNL	C1-B6	50	----	---	C5-B1	30	C5-B0	30
2B	SA	ORNL	C3-B0	50	----	---	C3-B9	30	C4-B6	40
2B	SA	ORNL	C1-B5	60	----	---	C5-B5	40	-----	---
3B	SA	ORNL	CC-1	0	CC-2	0	CC-1	0	CC-2	0
3B	SA	ORNL	C1-C9	50	C4-C0	20	C1-C5	10	C1-C0	10
3B	SA	ORNL	C4-C2	100	C1-C8	50	C2-C9	20	C3-C4	20
3B	SA	ORNL	C3-C1	150	C3-C0	100	C1-C2	50	C3-C6	50
3B	SA	ORNL	C2-C5	150	-----	---	C3-C7	100	C2-C7	50
3B	SA	ORNL	-----	---	-----	---	C3-C8	100	C4-C3	100
3B	SA	ORNL	-----	---	-----	---	C4-C9	150	-----	---
3B	SA	ORNL	-----	---	-----	---	C3-C3	150	-----	---
SA	SA	ORNL	S1A5-1	0	S1-A5	0	SXAX-1	0	SXAX-2	0
SA	SA	ORNL	S3-A7	10	S3-A5	20	S2-A3	10	S1-A0	10
SA	SA	ORNL	S1-A9	20	S2-A7	80	S2-A6	20	01	20
SA	SA	ORNL	S2-A5	20	----	---	S1-A6	50	S2-A4	50
SA	SA	ORNL	S2-A2	50	----	---	S3-A0	50	S2-A0	80
SA	SA	ORNL	S1-A8	100	----	---	S1-A2	80	S1-A1	100
SA	SA	ORNL	-----	---	----	---	S1-A7	100	-----	---
J-316	SA	JAERI	3S13-1	0	3S13-2	0	3S11-1	0	3S11-2	0
J-316	SA	JAERI	3S-01	100	3S-00	80	3S-04	100	3S-03	100
J-316	SA	JAERI	3S-08	180	3S-02	100	3S-07	120	3S-06	130
J-316	SA	JAERI	-----	---	3S-05	130	-----	---	-----	---
J-316	SA	JAERI	-----	---	3S-10	150	-----	---	-----	---
J-316	20% CW	JAERI	3C12-1	0	3C12-2	0	3C10-1	0	3C10-2	0
J-316	20% CW	JAERI	3C-11	100	3C-05	200	3C-03	200	3C-04	200
J-316	20% CW	JAERI	3C-08	200	3C-09	300	3C-06	350	3C-07	400
JPCA	SA	JAERI	PS14-1	0	PS14-2	0	PS11-1	0	PS11-2	0
JPCA	SA	JAERI	PS-01	100	PS-00	100	PS-03	100	PS-04	100
JPCA	SA	JAERI	PS-08	180	PS-02	130	PS-10	150	PS-07	150
JPCA	SA	JAERI	-----	---	PS-05	160	-----	---	-----	---
JPCA	SA	JAERI	-----	---	PS-09	180	-----	---	-----	---

[a]Tempered martensite.

ORNL-DWG 78-7701R

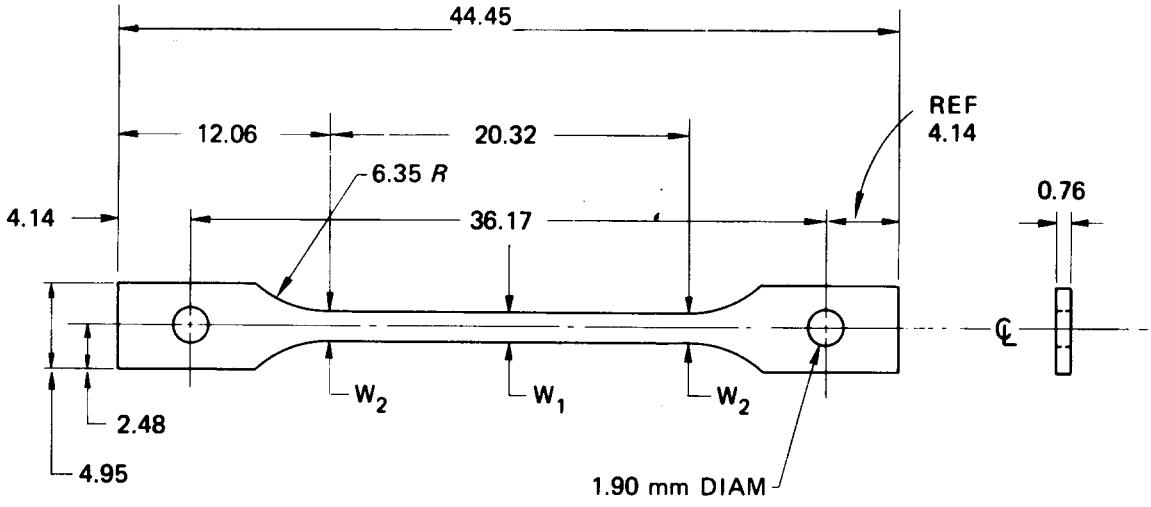

W_1 = 1.52 mm
W_2 = 0.025 TO 0.038 mm
GREATER THAN W_1

DIMENSIONS IN MILLIMETERS

Fig. 3.3. SS-1 tensile specimen.

ORNL-DWG 84-14010R

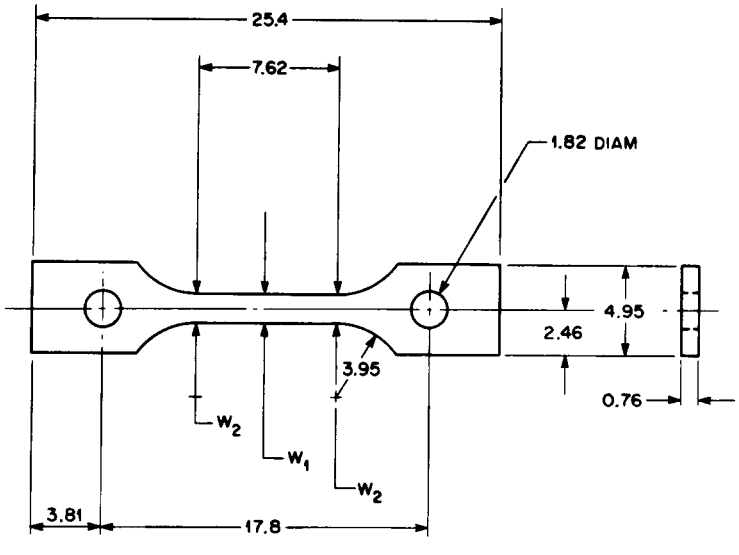

W_1 = 1.52 mm
W_2 = 0.025 TO 0.038 mm
GREATER THAN W_1

DIMENSIONS IN MILLIMETERS

Fig. 3.4. SS-3 tensile specimen.

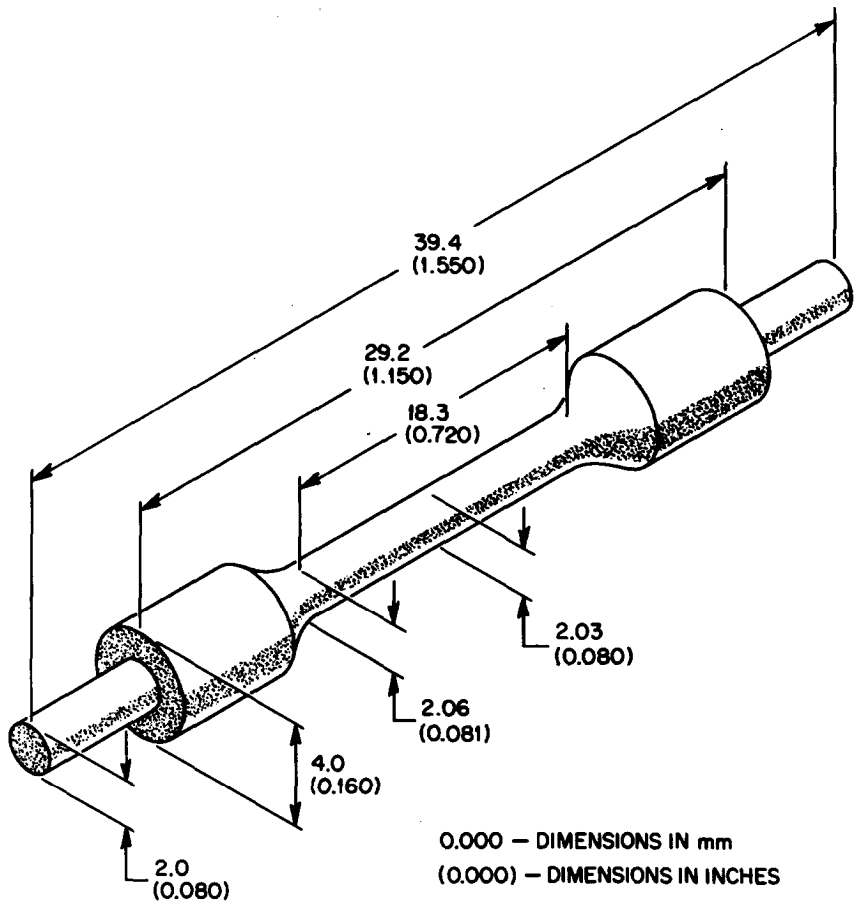

Fig. 3.5. HFIR submini tensile specimen.

3.6 CRACK-GROWTH SPECIMENS

The MFE-6J and -7J capsules contain crack-growth specimens from HEDL and JAERI. The specimen configuration is shown in Fig. 3.8, and the test matrix is presented in Tables 3.12 and 3.13. The specimen width shown in Fig. 3.8 does not apply to specimens being irradiated at 200°C. As a result of capsule design restraints, the width of these specimens is 10.16 mm. At all other temperatures the specimen width is 12.70 mm as shown.

Table 3.7. ORNL SS-1 tensile test matrix in MFE-6J and -7J capsules

Alloy	Condition	dpa	Specimen identification			
			60°C	200°C	330°C	400°C
316 SS	SA	10	AM-09	AM-04	AM-06	AM-12
316 SS	SA	10	AM-05	AM-10	AM-07	AM-08
316 SS	20% CW	10	B1-16	AM-22	AM-26	AM-25
316 SS	20% CW	10	B1-25	AM-28	AM-14	AM-13
316 SS	20% CW	10	B7-23	B5-5	AB-107	B1-17
316 SS	20% CW	10	C1-5	AB-26	B1-15	C1-10
316 SS	20% CW	10	B4-7	B1-5	B7-15	B5-12
316 SS	20% CW	10	AM-18	C1-17	B5-10	B7-21
316 SS	20% CW	10	AM-15	B7-9	B4-12	B7-2
316 SS	20% CW	10	----	B4-23	C1-23	B4-10
316 SS	20% CW	10	----	----	B7-22	B4-21
316 SS	20% CW	10	----	----	----	B5-23
316 SS	20% CW	10	----	----	----	AB-87
B1	SA	30	B1-08	B1-07	-----	-----
B2	SA	30	B2-08	B2-07	-----	-----
B3	SA	30	B3-08	B3-07	-----	-----
B5	SA	30	B5-08	B5-07	-----	-----
B6	SA	30	B6-08	B6-07	-----	-----
B7	SA	30	B7-08	B7-07	-----	-----
B9	SA	30	B9-08	B9-07	-----	-----
B10	SA	30	B10-08	B10-07	-----	-----
B11	SA	30	B11-08	B11-07	-----	-----
B12	SA	30	B12-08	B12-07	-----	-----
B13	SA	30	B13-08	B13-07	-----	-----
E-1	SA	30	E1-08	E1-07	-----	-----
E-2	SA	30	E2-08	E2-07	-----	-----
E-3	SA	30	E3-08	E3-07	-----	-----
E-4	SA	30	E4-08	E4-07	-----	-----
E-5	SA	30	E5-08	E5-07	-----	-----
E-6	SA	30	E6-08	E6-07	-----	-----
E-8	SA	30	E8-08	E8-07	-----	-----
E-9	SA	30	E9-08	E9-07	-----	-----
E-10	SA	30	E10-08	E10-07	-----	-----
E-11	SA	30	-----	E11-07	-----	-----
E-12	SA	30	-----	E12-07	-----	-----
E-13	SA	30	-----	E13-07	-----	-----
E-14	SA	30	-----	E14-07	-----	-----

Table 3.8. Test matrix of ORNL SS-3 tensile specimens in MFE-6J and -7J capsules

Alloy	Condition	dpa	Specimen Identification 60°C	200°C	330°C	400°C
PCA	25% CW	10	----	EK-33	-----	-----
PCA	25% CW	10	EK-18	EK-34	-----	-----
PCA	25% CW	10	EK-19	EK-35	-----	-----
PCA	25% CW	10	EK-20	EK-36	-----	-----
PCA	25% CW	20	EK-21	EK-37	-----	-----
PCA	25% CW	20	EK-22	EK-38	-----	-----
PCA	25% CW	20	EK-23	EK-39	-----	-----
PCA	25% CW	20	EK-25	EK-40	-----	-----
PCA	25% CW	30	EK-26	EK-41	-----	-----
PCA	25% CW	30	EK-27	EK-42	-----	-----
PCA	25% CW	30	EK-28	EK-43	-----	-----
PCA	25% CW	30	EK-31	EK-46	-----	-----
316	20% CW	10	AE-01	AE-19	-----	-----
316	20% CW	10	AE-02	AE-20	-----	-----
316	20% CW	10	AE-04	AE-22	-----	-----
316	20% CW	10	AE-05	AE-23	-----	-----
316	20% CW	20	AE-06	AE-25	-----	-----
316	20% CW	20	AE-07	AE-26	-----	-----
316	20% CW	20	AE-08	AE-28	-----	-----
316	20% CW	20	AE-12	AE-31	-----	-----
316	20% CW	30	AE-13	AE-32	-----	-----
316	20% CW	30	AE-14	AE-34	-----	-----
316	20% CW	30	AE-15	AE-35	-----	-----
316	20% CW	30	AE-17	AE-37	-----	-----
PCA	25% CW	30	EC-10	EC-00	-----	-----
PCA	25% CW	30	EC-11	EC-03	-----	-----
PCA	25% CW	30	EC-12	EC-06	-----	-----
PCA	25% CW	30	EC-13	EC-08	-----	-----
PCA	25% CW	30	EC-14	EC-09	-----	-----
PCA	25% CW	30	EC-15	EC-21	-----	-----
PCA	B3	30	EL-04	EL-00	-----	-----
PCA	B3	30	EL-07	EL-03	-----	-----
PCA-20	25% CW	30	HV-09	HV-00	-----	-----
PCA-20	25% CW	30	HV-11	HV-02	-----	-----
PCA-20	25% CW	30	HV-12	HV-03	-----	-----
PCA-20	25% CW	30	HV-15	HV-04	-----	-----
PCA-20	25% CW	30	HV-16	HV-07	-----	-----
PCA-20	25% CW	30	HV-17	HV-08	-----	-----
PCMA-6	20% CW	30	MH-09	MH-01	-----	-----
PCMA-6	20% CW	30	MH-10	MH-02	-----	-----
PCMA-6	20% CW	30	MH-11	MH-05	-----	-----
PCMA-6	20% CW	30	MH-12	MH-06	-----	-----
PCMA-6	20% CW	30	MH-13	MH-07	-----	-----
PCMA-6	20% CW	30	MH-16	MH-08	-----	-----

Alloy	Condition	dpa	Specimen Identification 60°C	200°C	330°C	400°C
Zr-1	Annealed	10	----	-----	1-01	-----
Zr-1	Annealed	10	----	-----	1-02	-----
Zr-1	Annealed	10	----	-----	1-03	-----
Zr-B1	Annealed	10	----	-----	B-101	-----
Zr-B1	Annealed	10	----	-----	B-102	-----
Zr-B1	Annealed	10	----	-----	B-103	-----
Zr-B2	Annealed	10	----	-----	B-201	-----
Zr-B2	Annealed	10	----	-----	B-202	-----
Zr-B2	Annealed	10	----	-----	B-203	-----
Zr-4	Annealed	10	----	-----	52-1	-----
Zr-4	Annealed	10	----	-----	52-2	-----
Zr4-Li3	Annealed	10	----	-----	6701	-----
Zr4-Li3	Annealed	10	----	-----	6702	-----
Fe-Ni-Cr	Annealed	10	----	-----	871	-----
Fe-Ni-Cr-Li2	Annealed	10	----	-----	6901	-----
Fe-Ni-Cr-Li2	Annealed	10	----	-----	6902	-----
Ni-1Si	Annealed	10	----	-----	----	2701
Ni-1Si	Annealed	10	----	-----	----	2702
Ni-1Ti	Annealed	10	----	-----	----	3001
Ni-1Ti	Annealed	10	----	-----	----	3002
Ni-1Al	Annealed	10	----	-----	----	2901
Ni-1Al	Annealed	10	----	-----	----	2902
Ni-8Si	Annealed	10	----	-----	----	2801
Ni-8Si	Annealed	10	----	-----	----	2802
Fe-Ni-Cr(1Si)	Annealed	10	----	-----	----	7101
Fe-Ni-Cr(1Si)	Annealed	10	----	-----	----	7102
Fe-Ni-Cr(1Ti)	Annealed	10	----	-----	----	7301
Fe-Ni-Cr(1Ti)	Annealed	10	----	-----	----	7302
Fe-Ni-Cr(1Al)	Annealed	10	----	-----	----	7201
Fe-Ni-Cr(1Al)	Annealed	10	----	-----	----	7202
Fe	Annealed	10	----	-----	----	75-1
Fe	Annealed	10	----	-----	----	75-2
Fe-Li2	Annealed	10	----	-----	----	77-1
Fe-Li2	Annealed	10	----	-----	----	77-2
Fe-LoB	Annealed	10	----	-----	----	8101
Fe-LoB	Annealed	10	----	-----	----	8102
Fe-HiB	Annealed	10	----	-----	----	8201
Fe-HiB	Annealed	10	----	-----	----	8202

Table 3.9. Test matrix of HEDL SS-3 tensile specimens in MFE-6J and -7J capsules

Alloy	Condition*	dpa	Specimen Identification 60°C	200°C	330°C	400°C
VO-2262	A	10	TE-15	TE-17	TE-11	TE-13
VO-2262	A	20	----	----	TE-12	TE-14
VO-2262	A	30	TE-16	TE-18	-----	-----
VO-2267	C	10	TL-15	TL-19	TL-11	TL-13
VO-2267	C	10	TL-16	TL-20	-----	-----
VO-2267	C	20	TL-17	TL-21	TL-12	TL-14
VO-2267	C	30	TL-18	TL-22	-----	-----
VO-2264	B	10	TM-15	TM-19	TM-11	TM-13
VO-2264	B	10	TM-16	TM-20	-----	-----
VO-2264	B	20	TM-17	TM-21	-----	-----
VO-2264	B	30	TM-18	TM-22	TM-12	TM-14
VO-2265	C	10	TN-15	TN-19	TN-11	TN-13
VO-2265	C	10	TN-16	TN-20	-----	-----
VO-2265	C	20	TN-17	TN-21	-----	-----
VO-2265	C	30	TN-18	TN-22	TN-12	TN-14
VO-2266	C	10	TP-15	TP-19	TP-11	TP-13
VO-2266	C	10	TP-16	TP-20	-----	-----
VO-2266	C	20	TP-17	TP-21	-----	-----
VO-2266	C	30	TP-18	TP-22	TP-12	TP-14
VO-2268	C	10	TR-09	TR-10	TR-11	TR-15
VO-2268	C	10	TR-19	TR-22	TR-12	TR-16
VO-2268	C	20	TR-20	TR-23	TR-13	TR-17
VO-2268	C	30	TR-21	TR-24	TR-14	TR-18

Alloy	Condition*	dpa	Specimen Identification 60°C	200°C	330°C	400°C
VO-2269	C	10	TU-07	TU-10	TU-11	TU-15
VO-2269	C	10	TU-19	TU-22	TU-12	TU-16
VO-2269	C	20	TU-09	TU-23	TU-13	TU-17
VO-2269	C	30	TU-21	TU-24	TU-14	TU-18
VO-2754	D	10	TW-11	TW-14	----	----
VO-2754	D	20	TW-12	TW-16	----	----
VO-2754	D	30	TW-13	TW-17	----	----
VO-2754	D	10	----	TW-15	----	----
VO-2755	D	10	TX-11	TX-15	----	----
VO-2755	D	10	TX-12	-----	----	----
VO-2755	D	20	TX-13	TX-16	----	----
VO-2755	D	30	TX-14	TX-17	----	----
UC-19	A	10	TZ-19	TZ-22	TZ-11	TZ-15
UC-19	A	20	----	-----	TZ-13	TZ-17
UC-19	A	30	TZ-21	TZ-23	TZ-14	TZ-18
UC-19	A	10	----	-----	TZ-12	TZ-16
VO-2702	D	10	----	----	TT-11	TT-15
VO-2702	D	10	----	----	TT-12	TT-16
VO-2702	D	20	----	----	TT-13	TT-17
VO-2702	D	30	----	----	TT-14	TT-18
VO-2700	D	10	----	----	TF-11	TF-15
VO-2700	D	10	----	----	TF-12	TF-16
VO-2700	D	20	----	----	TF-13	TF-17
VO-2700	D	30	----	----	TF-14	TF-18

*A = 900°C/20 h/WQ + 950°C/20 min/WQ + 650°C/2 h/AC.

B = 1000°C/20 h/AC + 1100°C/5 min/AC + 700°C/2 h/AC.

C = 1000°C/20 h/AC + 1100°C/10 min/AC + 700°C/2 h/AC.

D = 1000°C/20 h/AC + 1100°C/5 min/AC + 650°C/2 h/AC.

Table 3.10. JAERI tensile test matrix in MFE-6J and -7J capsules

Alloy	Condition	dpa	Specimen Identification 60°C	200°C	330°C	400°C
JPCA	15% CW	10	DL-36	DL-3	DL-7	DL-19
JPCA	15% CW	10	DL-37	DL-4	DL-8	DL-20
JPCA	15% CW	10	DL-38	DL-5	DL-9	DL-21
JPCA	15% CW	10	----	DL-6	DL-10	DL-22
JPCA	15% CW	10	----	DL-45	DL-11	DL-23
JPCA	15% CW	10	----	DL-46	DL-12	DL-24
JPCA	15% CW	20	DL-39	DL-47	DL-13	DL-25
JPCA	15% CW	20	DL-40	DL-48	DL-14	DL-26
JPCA	15% CW	20	DL-41	DL-49	DL-15	DL-27
JPCA	15% CW	30	DL-42	DL-50	DL-16	DL-28
JPCA	15% CW	30	DL-44	DL-52	DL-17	DL-29
JPCA	15% CW	30	----	DL-53	DL-18	DL-30
J316	20% CW	10	FL-31	FL-39	FL-13	FL-1
J316	20% CW	10	FL-32	FL-40	FL-14	FL-2
J316	20% CW	10	FL-33	FL-42	FL-15	FL-3
J316	20% CW	10	----	FL-43	FL-16	FL-4
J316	20% CW	10	----	FL-44	FL-17	FL-5
J316	20% CW	10	----	FL-55	FL-18	FL-6
J316	20% CW	20	FL-34	FL-46	FL-19	FL-7
J316	20% CW	20	FL-35	FL-47	FL-20	FL-8
J316	20% CW	20	FL-36	FL-50	FL-21	FL-9
J316	20% CW	30	FL-37	FL-51	FL-22	FL-10
J316	20% CW	30	FL-38	FL-52	FL-23	FL-11
J316	20% CW	30	----	FL-53	FL-24	FL-12
JPCA	15% CW	10	----	----	TE-29	----
JPCA	(HFIR type)	10	----	----	TE-30	----
JPCA	(HFIR type)	30	----	----	TE-31	----
JPCA	(HFIR type)	30	----	----	TE-32	----
JPCA	25% CW	10	GL-6	----	GL-1	----
JPCA	25% CW	10	GL-7	----	GL-2	----
JPCA	25% CW	10	GL-8	----	----	----
JPCA	25% CW	20	GL-9	----	----	----
JPCA	25% CW	20	GL-10	----	----	----
JPCA	25% CW	20	GL-11	----	----	----
JPCA	25% CW	30	GL-12	----	GL-3	----
JPCA	25% CW	30	GL-13	----	GL-4	----
JPCA	Aged	10	DLA-6	----	DLA-1	----
JPCA	Aged	10	DLA-7	----	DLA-2	----
JPCA	Aged	10	DLA-8	----	----	----
JPCA	Aged	20	DLA-10	----	----	----
JPCA	Aged	20	DLA-11	----	----	----
JPCA	Aged	20	DLA-12	----	----	----
JPCA	Aged	30	DLA-13	----	DLA-3	----
JPCA	Aged	30	DLA-14	----	DLA-4	----

Alloy	Condition	dpa	Specimen Identification 60°C	200°C	330°C	400°C
JPCA	SA	10	CL-3	CL-42	CL-7	CL-19
JPCA	SA	10	CL-4	CL-43	CL-8	CL-20
JPCA	SA	10	CL-5	CL-55	CL-9	CL-21
JPCA	SA	10	----	CL-46	CL-10	CL-22
JPCA	SA	10	----	CL-47	CL-11	CL-23
JPCA	SA	10	----	CL-48	CL-12	CL-24
JPCA	SA	20	CL-36	CL-49	CL-13	CL-25
JPCA	SA	20	CL-38	CL-50	CL-14	CL-26
JPCA	SA	20	CL-39	CL-51	CL-15	CL-27
JPCA	SA	30	CL-40	CL-52	CL-16	CL-28
JPCA	SA	30	CL-41	CL-53	CL-17	CL-29
JPCA	SA	30	----	CL-54	CL-18	CL-30
316 SS	SA	10	EL-33	EL-43	EL-1	EL-14
316 SS	SA	10	EL-34	EL-44	EL-2	EL-15
316 SS	SA	10	EL-36	EL-46	EL-3	EL-16
316 SS	SA	10	----	EL-47	EL-4	EL-17
316 SS	SA	10	----	EL-48	EL-5	EL-18
316 SS	SA	10	----	EL-49	EL-6	EL-19
316 SS	SA	20	EL-37	EL-50	EL-7	EL-20
316 SS	SA	20	EL-38	EL-51	EL-8	EL-21
316 SS	SA	20	EL-39	EL-52	EL-9	EL-22
316 SS	SA	30	EL-40	EL-53	EL-10	EL-23
316 SS	SA	30	EL-41	EL-54	EL-11	EL-24
316 SS	SA	30	----	EL-55	EL-12	EL-25
316 SS	SA	30	16	24	24	24
J316	SAR	10	HL-6	HL-8	HL-1	HL-3
J316	SAR	10	HL-7	HL-9	HL-2	HL-4
Dual Phase	SA	10	IL-6	IL-8	IL-1	IL-3
(K)	SA	10	IL-7	IL-9	IL-2	IL-4
All Martensite	Heat Tr.	10	ML-6	----	ML-1	ML-3
All Martensite	Heat Tr.	10	ML-7	----	ML-2	ML-4
J316	SA, TIG (W.J.)	10	ELW-1	ELW-3	----	----
J316	SA, TIG (W.J.)	10	ELW-2	----	----	----
J316	CW, TIG (W.J.)	10	FLW-1	FLW-7	----	----
J316	CW, TIG (W.J.)	10	FLW-6	----	----	----
J316	SA, EB (W.J.)	10	JL-6	JL-8	JL-1	JL-3
J316	SA, EB (W.J.)	10	JL-7	JL-9	JL-2	JL-4
J316	SA, TIG (Depo)	10	D-29	----	D-17	D-23
J316	SA, TIG (Depo)	10	D-30	----	D-19	D-24
J316	CW, TIG (Depo)	10	D-57	----	D-49	D-53
J316	CW, TIG (Depo)	10	D-58	----	D-50	D-54
JPCA	SA, TIG (Depo)	10	CLW-13	CLW-18	CLW-5	CLW-9
JPCA	SA, TIG (Depo)	10	CLW-14	----	CLW-6	CLW-10
JPCA	SA, TIG (Depo)	10	CLW-15	----	----	----
JPCA	SA, TIG (Depo)	10	CLW-16	----	----	----
JPCA	SA, EB (W.J.)	10	KL-6	KL-8	KL-1	KL-3
JPCA	SA, EB (W.J.)	10	KL-7	KL-9	KL-2	KL-4

ORNL-DWG 80-12052

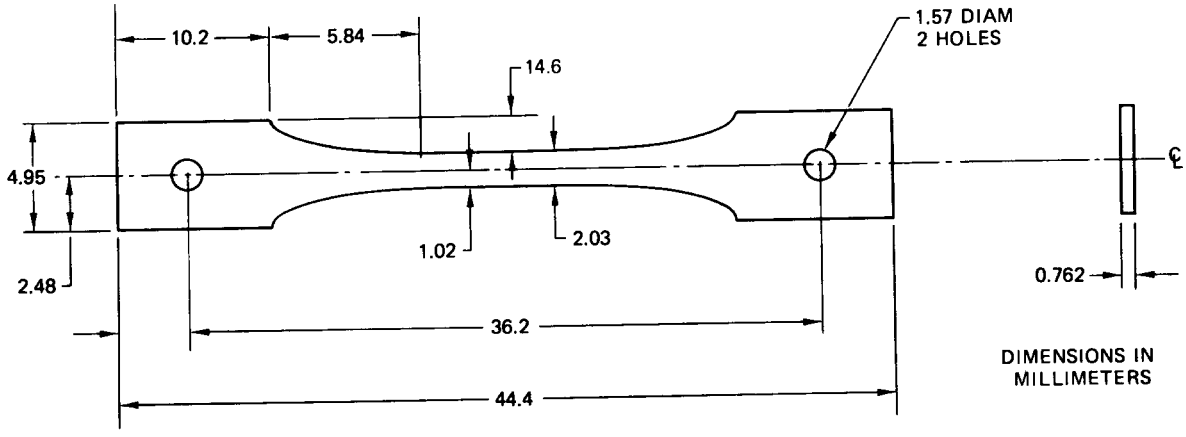

Fig. 3.6. Grodzinski fatigue specimen.

ORNL-DWG 81-4568

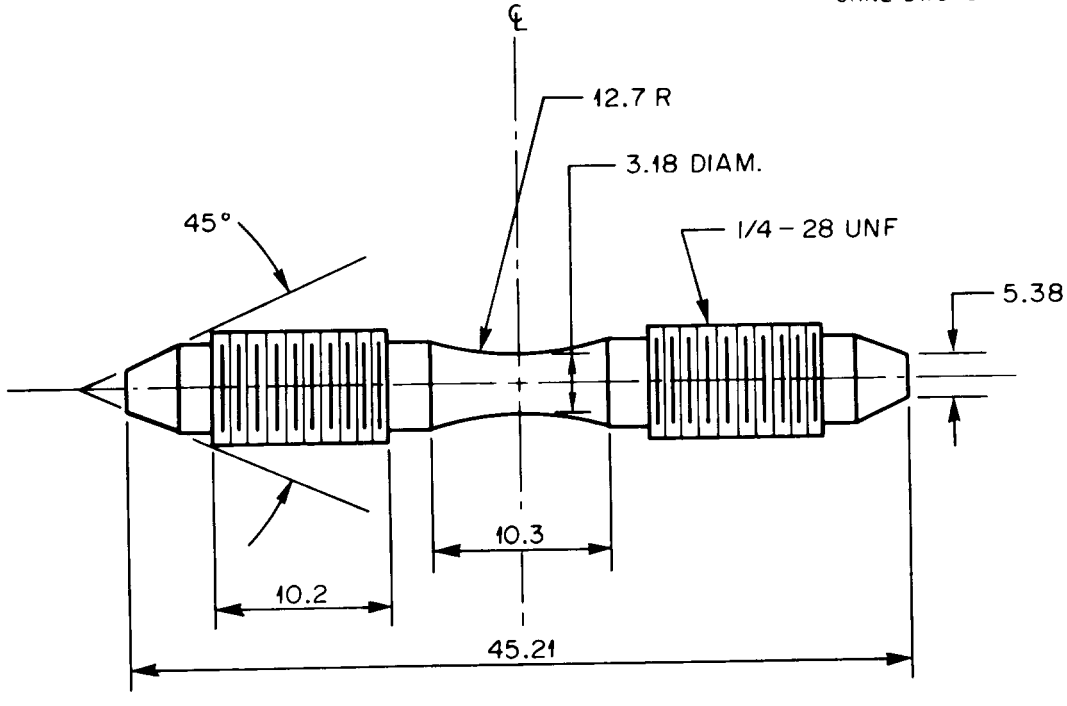

Fig. 3.7. Hourglass fatigue specimen; all dimensions are in millimeters.

Table 3.11. JAERI fatigue test matrix in MFE-6J and -7J capsules

Alloy	Condition	dpa	Specimen Identification			
			60°C	200°C	330°C	400°C
JPCA	15% CW	10	GFB-30	GFB-44	GFB-1	GFB-15
JPCA	15% CW	10	GFB-31	GFB-45	GFB-2	GFB-16
JPCA	15% CW	10	GFB-32	-----	GFB-3	GFB-17
JPCA	15% CW	10	GFB-33	-----	GFB-4	GFB-18
JPCA	15% CW	10	GFB-34	-----	GFB-5	GFB-19
JPCA	15% CW	10	GFB-35	-----	GFB-6	GFB-20
JPCA	15% CW	20	GFB-36	GFB-46	GFB-7	GFB-21
JPCA	15% CW	20	GFB-37	GFB-47	GFB-8	GFB-22
JPCA	15% CW	20	GFB-38	-----	GFB-9	-----
JPCA	15% CW	20	GFB-39	-----	GFB-10	-----
JPCA	15% CW	30	GFB-40	GFB-48	GFB-11	GFB-23
JPCA	15% CW	30	GFB-41	GFB-49	GFB-12	GFB-24
JPCA	15% CW	30	GFB-42	-----	GFB-13	-----
JPCA	15% CW	30	GFB-43	-----	GFB-14	-----
JPCA	15% CW	10	-----	-----	-----	FE-9
JPCA	Hourglass	10	-----	-----	-----	FE-17
JPCA	Hourglass	10	-----	-----	-----	FE-18
JPCA	15% CW	30	-----	-----	-----	FE-19
JPCA	Hourglass	30	-----	-----	-----	FE-31
JPCA	SA	10	GFA-30	GFA-44	GFA-1	GFA-15
JPCA	SA	10	GFA-31	GFA-45	GFA-2	GFA-16
JPCA	SA	10	GFA-32	-----	GFA-3	GFA-17
JPCA	SA	10	GFA-33	-----	GFA-4	GFA-18
JPCA	SA	10	GFA-34	-----	GFA-5	GFA-19
JPCA	SA	10	GFA-35	-----	GFA-6	GFA-20
JPCA	SA	20	GFA-36	GFA-46	GFA-7	GFA-21
JPCA	SA	20	GFA-37	GFA-47	GFA-8	GFA-22
JPCA	SA	20	GFA-38	-----	GFA-9	-----
JPCA	SA	20	GFA-39	-----	GFA-10	-----
JPCA	SA	30	GFA-40	GFA-48	GFA-11	GFA-23
JPCA	SA	30	GFA-41	GFA-49	GFA-12	GFA-24
JPCA	SA	30	GFA-42	-----	GFA-13	-----
JPCA	SA	30	GFA-43	-----	GFA-14	-----
J316	20% CW	10	GFD-30	GFD-44	GFD-1	GFD-15
J316	20% CW	10	GFD-31	GFD-45	GFD-2	GFD-16
J316	20% CW	10	GFD-32	-----	GFD-3	GFD-17
J316	20% CW	10	GFD-33	-----	GFD-4	GFD-18
J316	20% CW	10	GFD-34	-----	GFD-5	GFD-19
J316	20% CW	10	GFD-35	-----	GFD-6	GFD-20
J316	20% CW	20	GFD-36	GFD-46	GFD-7	GFD-21
J316	20% CW	20	GFD-37	GFD-48	GFD-8	GFD-22
J316	20% CW	20	GFD-38	-----	GFD-9	-----
J316	20% CW	20	GFD-39	-----	GFD-10	-----
J316	20% CW	30	GFD-40	GFD-49	GFD-11	GFD-23
J316	20% CW	30	GFD-41	GFD-50	GFD-12	GFD-24
J316	20% CW	30	GFD-42	-----	GFD-13	-----
J316	20% CW	30	GFD-43	-----	GFD-14	-----
J316	SA	10	GFC-30	GFC-44	GFC-1	GFC-15
J316	SA	10	GFC-31	GFC-45	GFC-2	GFC-16
J316	SA	10	GFC-32	-----	GFC-3	GFC-17
J316	SA	10	GFC-33	-----	GFC-4	GFC-18
J316	SA	10	GFC-34	-----	GFC-5	GFC-19
J316	SA	10	GFC-35	-----	GFC-6	GFC-20
J316	SA	20	GFC-36	GFC-46	GFC-7	GFC-21
J316	SA	20	GFC-37	GFC-47	GFC-8	GFC-22
J316	SA	20	GFC-38	-----	GFC-9	-----
J316	SA	20	GFC-39	-----	GFC-10	-----
J316	SA	30	GFC-40	GFC-48	GFC-11	GFC-23
J316	SA	30	GFC-41	GFC-49	GFC-12	GFC-24
J316	SA	30	GFC-42	-----	GFC-13	-----
J316	SA	30	GFC-43	-----	GFC-14	-----

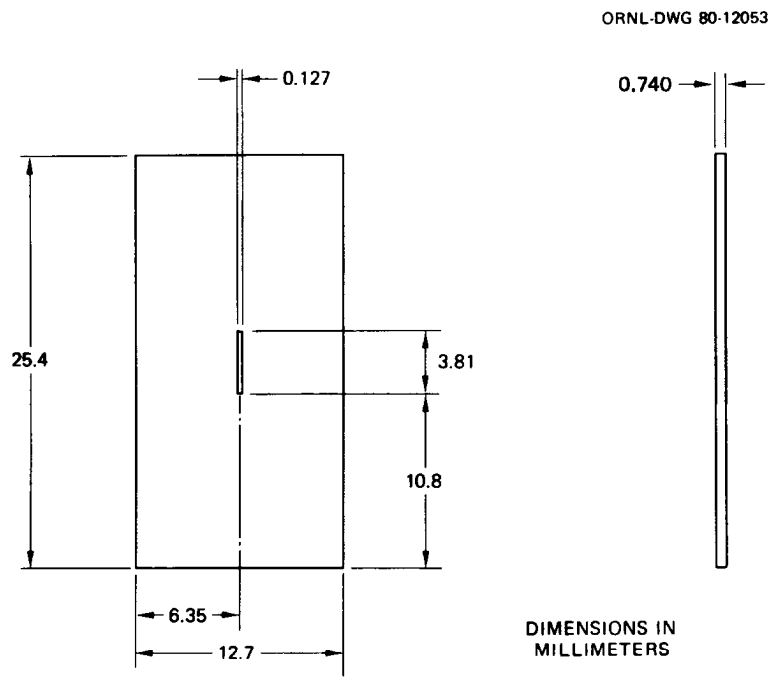

Fig. 3.8. Crack-growth specimen; tabs are welded along the 25.4-mm edge following irradiation.

Table 3.12. Test matrix of HEDL crack-growth specimens in MFE-6J capsule

Alloy	Condition	dpa	Specimen Identification	
			60°C	200°C
316 SS	20% CW	10	AH-01	AH-17
316 SS	20% CW	10	AH-02	AH-18
316 SS	20% CW	10	AH-03	--
316 SS	20% CW	20	AH-04	AH-19
316 SS	20% CW	20	AH-05	AH-20
316 SS	20% CW	20	AH-08	--
316 SS	20% CW	30	AH-09	AH-24
316 SS	20% CW	30	AH-14	AH-25
316 SS	20% CW	30	AH-15	--
PCA	25% CW	10	AT-01	AT-27
PCA	25% CW	10	AT-05	AT-28
PCA	25% CW	10	AT-07	AT-31
PCA	25% CW	20	AT-15	AT-32
PCA	25% CW	20	AT-16	AT-33
PCA	25% CW	20	AT-17	AT-36
PCA	25% CW	30	AT-19	AT-38
PCA	25% CW	30	AT-20	AT-39
PCA	25% CW	30	AT-24	--
HT-9	Tempered	30	--	EH-01
	Martensite	30	--	EH-03
		30	--	EH-09

Table 3.13. Description of JAERI crack-growth specimens in MFE-6J and -7J capsules

Alloy	Condition	dpa	Specimen identification			
			60°C	200°C	330°C	400°C
JPCA	15% CW	10	CGB-6	CGD-1	CGB-1	CGB-3
JPCA	15% CW	10	CGB-7	CGD-2	CGB-2	CGB-4
JPCA	15% CW	10	CGB-8	CGD-3	----	----
JPCA	15% CW	10	CGB-9	CGD-4	----	----
JPCA	15% CW	10	CGB-10	CGD-5	----	----
JPCA	15% CW	10	CGB-11	CGD-6	----	----
JPCA	SA	10	CGA-8	CGC-1	CGA-1	CGA-4
JPCA	SA	10	CGA-9	CGC-2	CGA-2	CGA-5
JPCA	SA	10	CGA-10	CGC-3	CGA-3	CGA-6
JPCA	SA	10	CGA-11	CGC-5	----	----
J316	20% CW	10	CGF-6	CGH-1	CGF-1	CGF-3
J316	20% CW	10	CGF-7	CGH-2	CGF-2	CGF-4
J316	20% CW	10	CGF-8	CGH-3	----	----
J316	20% CW	10	CGF-9	CGH-4	----	----
J316	SA	10	CGE-8	CGG-1	CGE-1	CGE-4
J316	SA	10	CGE-9	CGG-2	CGE-2	CGE-5
J316	SA	10	CGE-10	CGG-4	CGE-3	CGE-6
J316	SA	10	CGE-11	CGG-5	----	----

3.7 TEM DISKS

Transmission-electron-microscopy (TEM) disks are coin-shaped specimens 3 mm in diameter and 0.25 mm thick that are stacked as tightly as possible into tubular holders with inner diameters of 3.35 to 3.45 mm. The holders were made of type 6061 aluminum for the MFE-6J capsule and of type 304 stainless steel for the MFE-7J capsule. For purposes of identification and because of limited space availability, the TEM tube holders were of several different lengths, as shown in Table 3.14. Disk packets were scheduled for removal at the 10-, 20-, and 30-dpa levels. The ORNL TEM test matrix is given in Table 3.15, and the HEDL TEM test matrix is given in Tables 3.16 and 3.17. The JAERI test matrix consists of engineering alloys (Table 3.18) and base research alloys (Table 3.19).

Table 3.14. Test matrix of TEM disk packets in MFE-6J and -7J capsules

Source	Length (in.)	Holder Material	dpa	Specimen Identification			
				60°C	200°C	330°C	400°C
ORNL	0.65	Al	10	A	D	--	--
ORNL	0.65	Al	20	B	E	--	--
ORNL	0.65	Al	30	C	F	--	--
ORNL	0.50	Al	10	H	I	--	--
JAERI	1.00	Al	10	J1	J6	--	--
JAERI	1.00	Al	10	J2	J7	--	--
JAERI	1.00	Al	10	J3	J8	--	--
JAERI	1.00	Al	10	--	J9	--	--
JAERI	1.00	Al	10	--	J10	--	--
JAERI	1.00	Al	30	J4	J11	--	--
JAERI	1.00	Al	30	J5	J12	--	--
JAERI	1.00	SS	10	--	--	JP1	JP7
JAERI	1.00	SS	10	--	--	JP2	JP8
JAERI	1.00	SS	10	--	--	JP3	JP9
JAERI	1.00	SS	10	--	--	JP4	JP10
JAERI	1.00	SS	30	--	--	JP5	JP11
JAERI	1.00	SS	30	--	--	JP6	JP12
ORNL	0.75	SS	10	--	--	A	D
ORNL	0.75	SS	20	--	--	B	E
ORNL	0.75	SS	30	--	--	C	F
ORNL	0.75	SS	10	--	--	G	K
ORNL	0.75	SS	10	--	--	H	L
ORNL	0.75	SS	10	--	--	I	M
ORNL	0.75	SS	10	--	--	J	N
ORNL	0.75	SS	10	--	--	--	(Blank)
ORNL	0.50	SS	10	--	--	A	B
HEDL	0.75	SS	10	--	--	LB	LH
HEDL	0.75	SS	10	--	--	LB1	LH2
HEDL	0.75	SS	20	--	--	LE	LK
HEDL	0.75	SS	30	--	--	LF	LL

Table 3.15. ORNL TEM matrix for MFE-6J and -7J capsules

Alloy	Condition	Specimen Identification in Tube											
		MFE-6J						MFE-7J					
		60°C			200°C			330°C			400°C		
		A (10 dpa)	B (20 dpa)	C (30 dpa)	D (10 dpa)	E (20 dpa)	F (30 dpa)	A (10 dpa)	B (20 dpa)	C (30 dpa)	D (10 dpa)	E (20 dpa)	F (30 dpa)
PCA	25% CW	EC-101	EC-105	EC-108	EC-112	EC-115	EC-118	EC-01	EC-05	EC-09	EC-15	EC-27	EC-31
PCA	25% CW	EC-103	EC-107	EC-110	EC-114	EC-116	EC-119	EC-03	EC-07	EC-14	EC-25	EC-29	EC-34
HT-9	a	SA-25	SA-27	SA-29	SA-31	SA-33	SA-35	SA-37	SA-39	SA-41	SA-43	SA-45	SA-47
HT-9	a	SA-26	SA-28	SA-30	SA-32	SA-34	SA-36	SA-38	SA-40	SA-42	SA-44	SA-46	SA-48
1B	SA	1B-01	1B-03	1B-05	1B-07	1B-09	1B-11	1B-13	1B-15	1B-17	1B-19	1B-21	1B-23
1B	SA	1B-02	1B-04	1B-06	1B-08	1B-10	1B-12	1B-14	1B-16	1B-18	1B-20	1B-22	1B-24
2B	SA	2B-01	2B-03	2B-05	2B-07	2B-09	2B-11	2B-13	2B-15	2B-17	2B-19	2B-21	2B-23
2B	SA	2B-02	2B-04	2B-06	2B-08	2B-10	2B-12	2B-14	2B-16	2B-18	2B-20	2B-22	2B-24
3B	SA	3B-01	3B-03	3B-05	3B-07	3B-09	3B-11	3B-13	3B-15	3B-17	3B-19	3B-21	3B-23
SA	SA	3B-02	3B-04	3B-06	3B-08	3B-10	3B-12	3B-14	3B-16	3B-18	3B-20	3B-22	3B-24
SA	SA	S1-A9	S2-A2	SA-A4	S2-A6	S2-A8	S3-A1	S3-A4	S3-A6	S3-A8	S4-A0	S4-A2	S4-A4
SA	SA	S2-A0	S2-A3	S2-A5	S2-A7	S2-A9	S3-A3	S3-A5	SA-A7	SE-A9	S4-A1	S4-A3	S4-A5
B1	SA	B1-01	B1-03	B1-05	B1-07	B1-09	B1-11	B1-13	B1-15	B1-17	B1-19	B1-21	B1-23
B1	SA	B1-02	B1-04	B1-06	B1-08	B1-10	B1-12	B1-14	B1-16	B1-18	B1-20	B1-22	B1-24
B2	SA	B2-01	B2-03	B2-05	B2-07	B2-09	B2-11	B2-13	B2-15	B2-17	B2-19	B2-21	B2-23
B2	SA	B2-02	B2-04	B2-06	B2-08	B2-10	B2-12	B2-14	B2-16	B2-18	B2-20		
B3	SA	B3-01	B3-03	B3-05	B3-07	B3-09	B3-11	B3-13	B3-15	B3-17	B3-19	B3-21	B3-23
B3	SA	B3-02	B3-04	B3-06	B3-08	B3-10	B3-12	B3-14	B3-16	B3-18	B3-20	B3-22	B3-24
B5	SA	B5-01	B5-03	B5-05	----	----	----	B5-07	B5-09	B5-11	B5-13	B5-15	B5-17
B5	SA	B5-02	B5-04	B5-06	----	----	----	B5-08	B5-10	B5-12	B5-14	B5-16	B5-18
B10	SA	BA-01	BA-03	BA-05	----	----	----	BA-07	BA-09	BA-11	BA-13	BA-15	BA-17
B10	SA	BA-02	BA-04	BA-06	----	----	----	BA-08	BA-10	BA-12	BA-14	BA-16	BA-18
B11	SA	BB-01	BB-03	BB-05	BB-07	BB-09	BB-11	BB-13	BB-15	BB-17	BB-19	BB-21	BB-23
B11	SA	BB-02	BB-04	BB-06	BB-08	BB-10	BB-12	BB-14	BB-16	BB-18	BB-20	BB-22	BB-24
M1	SA	M1-01	M1-03	M1-05	M1-07	M1-09	M1-11	M1-13	M1-15	M1-17	M1-19	M1-21	M1-23
M1	SA	M1-02	M1-04	M1-06	M1-08	M1-10	M1-12	M1-14	M1-16	M1-18	M1-20	M1-22	M1-24
M3	SA	M3-01	M3-03	M3-05	M3-07	M3-09	M3-11	M3-13	M3-15	M3-17	M3-19	M3-21	M3-23
M3	SA	M3-02	M3-04	M3-06	M3-08	M3-10	M3-12	M3-14	M3-16	M3-18	M3-20	M3-22	M3-24
M4	SA	M4-01	M4-03	M4-05	----	----	----	M4-07	M4-09	M4-11	M4-13	M4-15	M4-17
M4	SA	M4-02	M4-04	M4-06	----	----	----	M4-08	M4-10	M4-12	M4-14	M4-16	M4-18
M6	SA	M6-01	M6-03	M6-05	M6-07	M6-09	M6-11	M6-13	M6-15	M6-17	M6-19	M6-21	M6-23
M6	SA	M6-02	M6-04	M6-06	M6-08	M6-10	M6-12	M6-14	M6-16	M6-18	M6-20	M6-22	M6-24
M9	SA	M9-01	M9-03	M9-05	----	----	----	M9-07	M9-09	M9-11	M9-13	M9-15	M9-17
M9	SA	M9-02	M9-04	M9-06	----	----	----	M9-08	M9-10	M9-12	M9-14	M9-16	M9-18
M11	SA	MA-01	MA-03	MA-05	----	----	----	MA-07	MA-09	MA-11	MA-13	MA-15	MA-17
M11	SA	MA-02	MA-04	MA-06	----	----	----	MA-08	MA-10	MA-12	MA-14	MA-16	MA-18
C	SA	----	----	----	X1-C0	X1-C3	X1-C5	X1-C7	X1-C9	X2-C1	X2-C3	X2-C5	X2-C8
C	SA	----	----	----	X1-C2	X1-C4	X1-C6	X1-C8	X2-C0	X2-C2	X2-C4	X2-C6	X2-C9
D	SA	----	----	----	X1-D0	X1-D2	X1-D4	X1-D7	X1-D9	X2-D1	X2-D3	X2-D8	X3-D1
D	SA	----	----	----	X1-D1	X1-D3	X1-D6	X1-D8	X2-D0	X2-D2	X2-D5	X2-D9	X3-D2
E	SA	----	----	----	X1-E0	X1-E2	X1-E4	X1-E6	X1-E8	X2-E0	X2-E2	X2-E4	X2-E6
E	SA	----	----	----	X1-E1	X1-E3	X1-E5	X1-E7	X1-E9	X2-E1	X2-E3	X2-E5	X2-E7
H	SA	----	----	----	X1-H0	X1-H2	X1-H5	X1-H7	X2-H2	X2-H5	X2-H7	X2-H0	X3-H2
H	SA	----	----	----	X1-H1	X1-H3	X1-H6	X2-H0	X2-H4	X2-H6	X2-H8	X3-H1	H3-H3
K	SA	----	----	----	----	----	----	X1-K9	X1-K4	X1-K6	X2-K9	X1-K0	X1-K5
K	SA	----	----	----	----	----	----	X2-K7	X3-K1	X1-K3	X1-K7	X2-K3	X3-K4
L	SA	----	----	----	----	----	----	X2-L0	X2-L6	X2-L9	X1-L7	X3-L2	X1-L1
L	SA	----	----	----	----	----	----	X2-L7	X3-L0	X2-L4	X1-L0	X3-L3	X2-L8
M	SA	----	----	----	X1-M0	X1-M2	X1-M4	X1-M7	X1-M9	X2-M1	X2-M3	X2-M6	X2-M8
M	SA	----	----	----	X1-M1	X1-M3	X1-M5	X1-M8	X2-M0	X2-M2	X2-M4	X2-M7	X2-M9
P	SA	----	----	----	X1-P0	X1-P2	X1-P6	X1-P9	X2-P1	X2-P3	X2-P6	X2-P8	X3-P0
P	SA	----	----	----	X1-P1	X1-P3	X1-P8	X2-P0	X2-P2	X2-P5	X2-P7	X2-P9	X3-P1

[a]Tempered martensite.

Table 3.16. HEDL TEM matrix for MFE-6J

Alloy	Condi-tion	Specimen identification					
		60°C			200°C		
		A (10 dpa)	B (20 dpa)	C (30 dpa)	D (10 dpa)	E (20 dpa)	F (30 dpa)
E90	SA	T9L4	T9L5	T9L6	T9L7	T9L9	T9MA
E20	SA	UBL4	UBL5	UBL6	UBL7	UBL9	UBMA
E22	SA	UEL4	UEL5	UEL6	UEL7	UEL9	EUMA
E23	SA	UFL4	UFL5	UFL6	UFL7	UFL9	UFMA
R58	SA	UHL4	UHL5	UHL6	UHL7	UHL9	UHMA
E37	SA	UKL4	UKL5	UKL6	UKL7	UKL9	UKMA
GE5	SA	BBL4	BBL5	BBL6	BBL7	BBL9	BBMA
E38	SA	UNL4	UNL5	UNL5	UNL7	UNL9	UNMA

3.8 CAPSULE ASSEMBLY

The original schedule called for the MFE-7J capsule to be assembled in March 1985 and installed in the ORR in April. The second capsule, MFE-6J, was to be assembled in June 1985 and installed in July. Prior to capsule assembly the specimens had to be placed in the specimen holders. The specimens, basket parts, and flux monitors for the MFE-7J capsule are shown in Fig. 3.9. The specimens had to be positioned in the baskets so that the specimen mass per unit length did not exceed 24.1 g/cm, a limit set by the maximum allowable gamma heating rate. Assembled baskets are shown in Fig. 3.10.

During final capsule assembly a leak developed in the primary bulkhead. The capsule was partially disassembled to repair the leak and then reassembled. The repairs caused the insertion date to be delayed until June 27, 1985. In addition, two thermocouples were lost: TE2, measuring the temperature in the middle of the 330°C region, and TE6 at the bottom of the 400°C region. Fortunately, there was enough redundancy in capsule instrumentation so that alternate thermocouples in the central spine could measure each region.

The MFE-6J capsule was assembled by a different team simultaneously with the MFE-7J capsule. The specimens were loaded into the appropriate

Table 3.17. HEDL TEM matrix for MFE-7J

Alloy	Condition[a]	Specimen Identification in Tube							
		330°C				400°C			
		LB (10 dpa)	LB-1 (10 dpa)	LE (20 dpa)	LF (30 dpa)	LH (10 dpa)	LH-2 (10 dpa)	LK (20 dpa)	LL (30 dpa)
E18	SA	LBT7	LBT7	LET7	LFT7	LHT7	LHT7	LKT7	LLT7
E18	SA	LBT7	LBT7	LET7	LFT7	LHT7	LHT7	LKT7	LLT7
E90	SA	LBT9	LBT9	LET9	LFT9	LHT9	LHT9	LKT7	LLT7
E90	SA	LBT9	LBT9	LET9	LFT9	LHT9	LHT9	LKT9	LLT9
E19	SA	LBUA	LBUA	LEUA	LFUA	LHUA	LHUA	LKUA	LLUA
E19	SA	LBUA	LBUA	LEUA	LFUA	LHUA	LHUA	LKUA	LLUA
E20	SA	LBUB	LBUB	LEUB	LFUB	LHUB	LHUB	LKUB	LLUB
E20	SA	LBUB	LBUB	LEUB	LFUB	LHUB	LHUB	LKUB	LLUB
E22	SA	LBUE	LBUE	LEUE	LFUB	LHUE	LHUE	LKUE	LLUE
E22	SA	LBUE	LBUE	LEUE	LFUE	LHUE	LHUE	LKUE	LLUE
E23	SA	LBUF	LBUF	LEUF	LFUF	LHUF	LHUF	LKUF	LLUF
E23	SA	LBUF	LBUF	LEUF	LFUF	LHUF	LHUF	LKUF	LLUF
R58	SA	LBUH	LBUH	LEUH	LFUH	LHUH	LHUH	LKUH	LLUH
R58	SA	LBUH	LBUH	LEUH	LFUH	LHUH	LHUH	LKUH	LLUH
E37	SA	LBUK	LBUK	LEUK	LFUK	LHUK	LHUK	LKUK	LLUK
E37	SA	LBUK	LBUK	LEUK	LFUK	LHUK	LHUK	LKUJ	LLUK
E37	20% cold work	LBBH	LBBH	LEBH	LFBH	LHBH	LHBH	LKBH	LLBH
GE29	SA	LBUM	LBUM	LEUM	LFUM	LHUM	LHUM	LKUM	LLUM
GE29	SA	LBUM	LBUM	LEUM	LFUM	LHUM	LHUM	LKUM	LLUM
R41	SA	LBUO	LBUO	LEUO	LFUO	LHUO	LHUO	LKUO	LLUO
E38	SA	LBUN	LBUN	LEUN	LFUN	LHUN	LHUN	LKUN	LLUN
GE10	SA	LBBP	LBBP	LEBP	LFBP	LHBP	LHBP	LKBP	LLBP
GE10	SA	LBBP	LBBP	LEBP	LFBP	LHBP	LHBP	LKBP	LLBP
GE5	SA	LBBB	LBBB	LEBB	LFBB	LHBB	LHBB	LKBB	LLBB
GE5	SA	LBBB	LBBB	LEBB	LFBB	LHBB	LHBB	LKBB	LLBB
R72	SA	LBFE	LBFE	LEFE	LFFE	LHFF	LHFF	LKFF	LLFF
GE26	SA	LBUL	LBUL	LEUL	LFUL	LHUL	LHUL	LKUL	LLUL
GE26	SA	LBUL	LBUL	LEUL	LFUL	LHUL	LHUL	LKUL	LLUL
R48	SA	LBUP	LBUP	LEUP	LFUP	LHUP	LHUP	LKUP	LLUP
316	SA	LBNB	LBNB	LENB	LFNB	LHNB	LHNB	LKNB	LLNB
R73	SA	LBFK	LBFK	LEFK	LFFK	LHFK	LHFK	LKFK	LLFK
R76	SA	LBUR	LBUR	LEUR	LFUR	LHUR	LHUR	LKUR	LLUR
R83	SA	LBUT	LBUT	LEUT	LFUT	LHUT	LHUT	LKUT	LLUT
R67	SA	LBE4	LBE4	LEE4	LFE4	LHE4	LHE4	LKE4	LLE4
R69	SA	LBE9	LBE9	LEE9	LFE9	LHE9	LHE9	LKE9	LLE9
R70	SA	LBFA	LBFA	LEFA	LFFA	LHFA	LHFA	LKFA	LLFA
R71	SA	LBFB	LBFB	LEFB	LFFB	LHFB	LHFB	LKFB	LLFB
R66	SA	LBE3	LBE3	LEE3	LFE3	LHE3	LHE3	LKE3	LLE3
R74	SA	LBFL	LBFL	LEFL	LFFL	LHFL	LHFL	LKFL	LLFL

Table 3.17. (continued)

Alloy	Condition[a]	Specimen Identification in Tube							
		330°C				400°C			
		LB (10 dpa)	LB-1 (10 dpa)	LE (20 dpa)	LF (30 dpa)	LH (10 dpa)	LH-2 (10 dpa)	LK (20 dpa)	LL (30 dpa)
R87	SA	LBUU	LBUU	LEUU	LFUU	LHUU	LHUU	LKUO	LLUO
R75	SA	LBFM	LBFM	LEFM	LFFM	LHFM	LHFM	LKFM	LLFM
10998	D	LBPZ	LBPZ	LEPZ	LFPZ	LHPZ	LHPZ	LKPZ	LLPZ
HT-9	B	LBRF	LBRF	LERF	LFRF	LHRF	LHRF	LKRF	LLRF
10996	D	LBPV	LBPV	LEPV	LFPV	LHPV	LHPV	LKPV	LLPV
VO-2263	A	LBP4	LBP4	LEP4	LFP4	LHP4	LHP4	LKP4	LLP4
VO-2262	A	LBP3	LBP3	LEP3	LFP3	LHP3	LHP3	LKP3	LLP3
VO-2264	B	LBP6	LBP6	LEP6	LFP6	LHP6	LHP6	LKP6	LLP6
UC-19	A	LBP5	LBP5	LEP5	LFP5	LHP5	LHP5	LKP5	LLP5
VO-2265	C	LBP7	LBP7	LEP7	LFP7	LHP7	LHP7	LKP7	LLP7
VO-2268	C	LBRB	LBRB	LERB	LFRB	LHRB	LHRB	LKRB	LLRB
VO-2267	C	LBRA	LBRA	LERA	LFRA	LHRA	LHRA	LKRA	LLRA
VO-2269	C	LBRE	LBRE	LERE	LFRE	LHRE	LHRE	LKRE	LLRE
E38	SA	LBUN	LBUN	LEUN	LFUN	LHUN	LHUN	LKUN	LLUN
R41	SA	LBUO	LBUO	LEUO	LFUO	LHUO	LHUO	LKUO	LLUO
R48	SA	LBUP	LBUP	LEUP	LFUP	LHUP	LHUP	LKUP	LLUP
R72	SA	LBFE	LBFE	LEFE	LFFE	LHFE	LHFE	LKFE	LLFE
R73	SA	LBFK	LBFK	LEFK	LFFK	LHFK	LHFK	LKFK	LLFK
R74	SA	LBFL	LBFL	LEFL	LFFL	LHFL	LHFL	LKFL	LLFL
R76	SA	LBUR	LBUR	LEUR	LFUR	LHUR	LHUR	LKUR	LLUR
R66	SA	LBE3	LBE3	LEE3	LFE3	LHE3	LHE3	LKE3	LLE3
R83	SA	LBUT	LBUT	LEUT	LFUT	LHUT	LHUT	LKUT	LLUT
VO-2266	C	LBP9	LBP9	LEP9	LFP9	LHP9	LHP9	LKP9	LLP9
R67	SA	LBE4	LBE4	LEE4	LFE4	LHE4	LHE4	LKE4	LLE4

[a]SA: 1030°C/30 min/AC.
A: 900°C/20 h/WQ + 950°C/20 min/WQ + 650°C/2 h/AC.
B: 1000°C/20 h/AC + 1100°C/5 min/AC + 700°C/2 h/AC.
C: 1000°C/20 h/AC + 1100°C/10 min/AC + 700°C/2 h/AC.
D: 1000°C/20 h/AC + 1100°C/30 min/AC + 700°C/2 h/AC.

Table 3.18. JAERI engineering alloy TEM matrix in MFE-6J and -7J

Alloy	Condition[a]	Abbreviated Name	Identification of Tubes Containing Alloy			
			60	200	330	400
JPCA	SA 1175°C	PS1	J1, J4	J6, J11	J1, J5	J7, J11
JPCA	SA 1100°C	PS2	J1, J4	J6, J11	J1, J5	J7, J11
JPCA	SA 1050°C	PS3	J1, J4	J6, J11	J1, J5	J7, J11
JPCA	PS2 + 10% cold work	PC1	J1, J4	J6, J11	J1, J5	J7, J11
JPCA	PS2 + 20% cold work	PC3	J1, J4	J6, J11	J1, J5	J7, J11
C	SA 1100°C	CS1	J1, J4	J6, J11	J1, J5	J7, J11
C	CS1 + 20% cold work	CC1	J1, J4	J6, J11	J1, J5	J7, J11
K	SA 1050°C	KS1	J1, J4	J6, J11	J1, J5	J7, J11
K	KS1 + 20% cold work	KC1	J1, J4	J6, J11	J1, J5	J7, J11
J316	SA 1050°C	SS1	J1, J4	J6, J11	J1, J5	J7, J11
J316	SS1 + 20% cold work	SC1	J1, J4	J6, J11	J1, J5	J7, J11
Aged JPCA	PC3 + 2 h at 800°C	PA1	J1, J4	J6, J11	J1, J5	J7, J11
Aged JPCA	PC3 + 8 h at 800°C	PA2	J2, J4	J7, J12	J2, J6	J8, J12
High Ni Alloy I	SA 1100°C	Ist	J2, J4	J7, J12	J2, J6	J8, J12
High Ni Alloy I	Ist + 3000 h at 700°C	Iag	J2, J4	J7, J12	J2, J6	J8, J12
High Ni Alloy Q	SA 1100°C	Qst	J2, J5	J7, J12	J2, J6	J8, J12
High Ni Alloy Q	Qst + 3000 h at 700°C	Qag	J2, J5	J7, J12	J2, J6	J8, J12
Ferritic Steel	SA 1050°C + AC	FD1	J2, J5	J7, J12	J2, J6	J8, J12
Ferritic Steel	FD1 + 1 h at 775°C	FD2	J2, J5	J7, J12	J2, J6	J8, J12
HT-9	SA 1050°C + AC + 1 h at 780°C	FD3	J2, J5	J7, J12	J2, J6	J8, J12
J316 TIG weld	Matrix	SW1	J5	J8	J3	J9
J316 TIG weld	HAZ	SW2	J5	J8	J3	J9
J316 TIG weld	Bond	SW3	J5	J8	J3	J9
J316 TIG weld	Deposit	SW4	J5	J8	J3	J9
SAR (type 304)	A	SR1	J2, J5	J7, J12	J2, J6	J8, J12
SAR (type 316)	B	SR2	J2, J5	J7, J12	J2, J6	J8, J12
High Mn 1	SA 1050°C	MS1	J3	J9	J4	J10
High Mn 2	SA 1050°C	MS2	J3	J9	J4	J10
SN 1	SA 1050°C	SA1	----	J7, J12	J2, J6	J8, J12
SN 5	SA 1050°C	DP1	J2, J5	J7, J12	J2, J6	J8, J12
Dual phase A	SA 1050°C	DP2	J3	J8	J3	J9
Dual phase B	SA 1050°C	DP3	J3	J8	J3	J9
Dual phase C	SA 1050°C	DP4	J3	J8	J3	J9
Dual phase D	SA 1100°C	DP5	J3	J8	J3	J9
Dual phase E	SA 1050°C	DP6	J3	J9	J3, J4	J9, J10
Dual phase K	SA 1050°C	DP7	J3	----	J4	J10
Dual phase G	SA + 5 h at 1200°C	DP8	J2	J9	J4	J10
Dual phase I	SA + 4 h at 1200°C	DP9	J2	J9	J4	J10
Dual phase J	SA + 1 h at 1200°C	DP10	J3	J9	J4	J10
All martensite	C	AM1	J4	J9	----	J7, J11
Incoloy 800	SA at 1120°C	IN1	J4	J9	----	J7, J11
HP 12 Ni	SA at 1200°C	HP1	J4	J9	----	J7, J11
HP 35 Ni	SA at 1200°C	HP2	J4	J9	----	J7, J11
HP 50 Ni	SA at 1200°C	HP3	J4	J9	----	J8, J11

[a]A: SA — 1080°C + 50% CW + 15 h at 575°C + 5 h at 775°C.
B: SA — 1150°C + 50% CW + 15 h at 650°C + 5 h at 775°C.
C: SA — 1050°C + AC + 1 h at 775°C + AC.

Table 3.19. JAERI basic research TEM test matrix in MFE-6J and -7J

Alloy Composition	Condition	Abbre-viated Name	Identification of Tubes Containing Alloy			
			(60°C)	(200°C)	(330°C)	(400°C)
Fe–0.055C–0.53Si–1.88Mn–0.024P–0.009S–15.27Ni–15.80Cr–2.66Mo–0.24Ti–0.0032B–0.0039N	20% CW	UP1	J3	J10	J4	J10
Fe–0.056C–0.74Si–0.20Mn–0.008P–0.006S–1.37Ni–8.86Cr–2.46Mo–0.06Nb–0.0069N	SA 1050°C + 1 h 775°C	UF1	J3	J10	J4	J10
Fe–22Cr–5.5Ni–3Mo–0.1N–0.02C	SA 1050°C	UI1	J3	J10	J4	J10
Fe–14.5Cr–16Ni–2.5Mo–0.006N–0.003C	SA 1050°C	UI2	J3	J10	J4	J10
Fe–14.5Cr–16Ni–2.5Mo–0.007N–0.054C	SA 1050°C	UI3	J3	J10	J4	J10
Fe–14.5Cr–16Ni–2.5Mo–0.076N–0.061C	SA 1050°C	UI4	J3	J10	J4	J10
Fe–16Cr–15Ni–2.5Mo–0.008N–0.001C–0.1P	SA 1050°C	UI5	J3	J10	J4	J10
Fe–9Cr–1Mo–0.2Zr–0.05Y	SA 1000°C + 1 h 780°C	UY1	J3	J10	J4	J10
Fe–9Cr–1Mo–0.2Zr–0.2V–0.05Y	SA 1000°C + 1 h 780°C	UY2	J3	J10	J4	J10
Fe–9Cr–2.Mo–0.2Zr–0.2V–0.05Y	SA 1000°C + 1 h 780°C	UY3	J3	J10	J4	J10
Fe–9Cr–2Mo–0.2Zr–0.05Y	SA 1000°C + 1 h 780°C	UY4	J3	J10	J4	J10
Fe–7Cr–1.5Mo–0.2Zr–0.2V–0.05Y	SA 1000°C + 1 h 780°C	UY5	J3	J10	J4	J10
Fe–15Cr–16Ni	SA 1050°C	UK1	J3	J10	J4	J10
Fe–15Cr–16Ni–0.25Ti	SA 1050°C	UK2	J3	J10	J4	J10
Fe–15Cr–16Ni–0.25Ti–0.06C	SA 1175°C	UK3	J3	J10	J4	J10
Fe–15Cr–16Ni–0.06C	SA 1050°C	UN1	J3	J10	J4	J10
Fe–15Cr–16Ni–0.2Nb–0.06C	SA 1050°C	UN2	J3	J10	J4	J10
Fe–15Cr–16Ni–0.1Nb–0.06C	SA 1050°C	UN3	J3	J10	J4	J10
Fe	SA	UA1	J3	J10	J4	J10
Ni	SA	UA2	J3	J10	J4	J10
Cu	SA	UA3	J3	J10	J4	J10
Au	SA	UA4	J3	J10	J4	J10
Al	SA	UA5	J3	J10	J4	J10
Mo	SA	UA6	J3	J10	J4	J10
Nb	SA	UA7	J3	J10	J4	J10
Al–0.1 at. % Si	SA	UB1	J3	J10	J4	J10
Cu–0.2Ni	SA	UB2	J3	J10	J4	J10
Ni–0.2Cu	SA	UB3	J3	J10	J4	J10
Al–0.1 at. % Mg	SA	UB4	J3	J10	J4	J10
Al–0.1 at. % Li	SA	UB5	J3	J10	J4	J10
Al–0.1 at. % Mn	SA	UB6	J3	J10	J4	J10
V	SA 1000°C	UT1	J3	J10	J4	J10
V–0.2Ti	SA 1000°C	UT2	J3	J10	J4	J10
Fe–31Ni–3Ti	SA 1000°C	UU1	J3	J10	J4	J10

ORNL PHOTO 2367-85

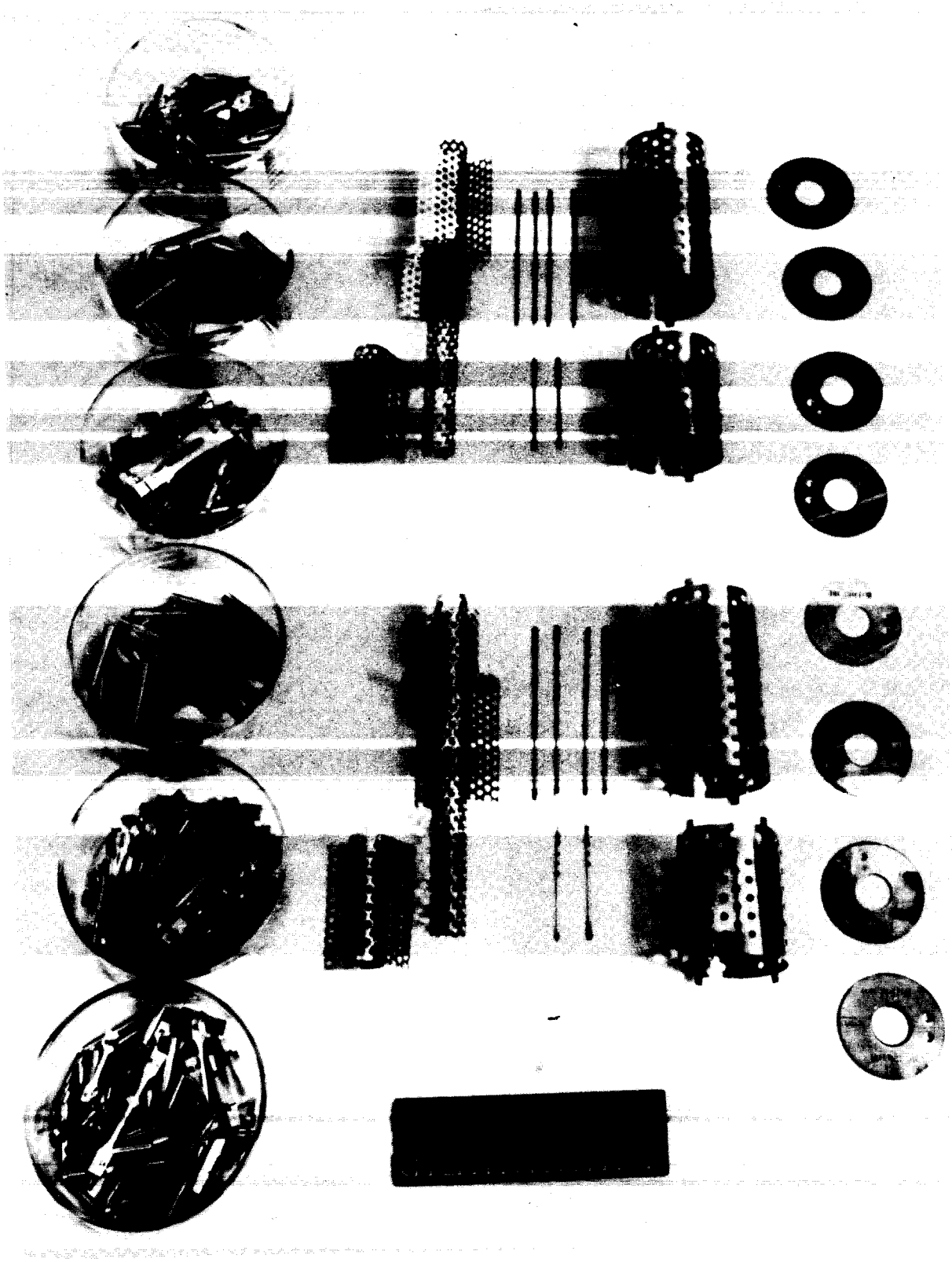

Fig. 3.9. ORR spectral-tailoring capsule MFE-7J specimens prior to assembly.

ORNL PHOTO 2366-85

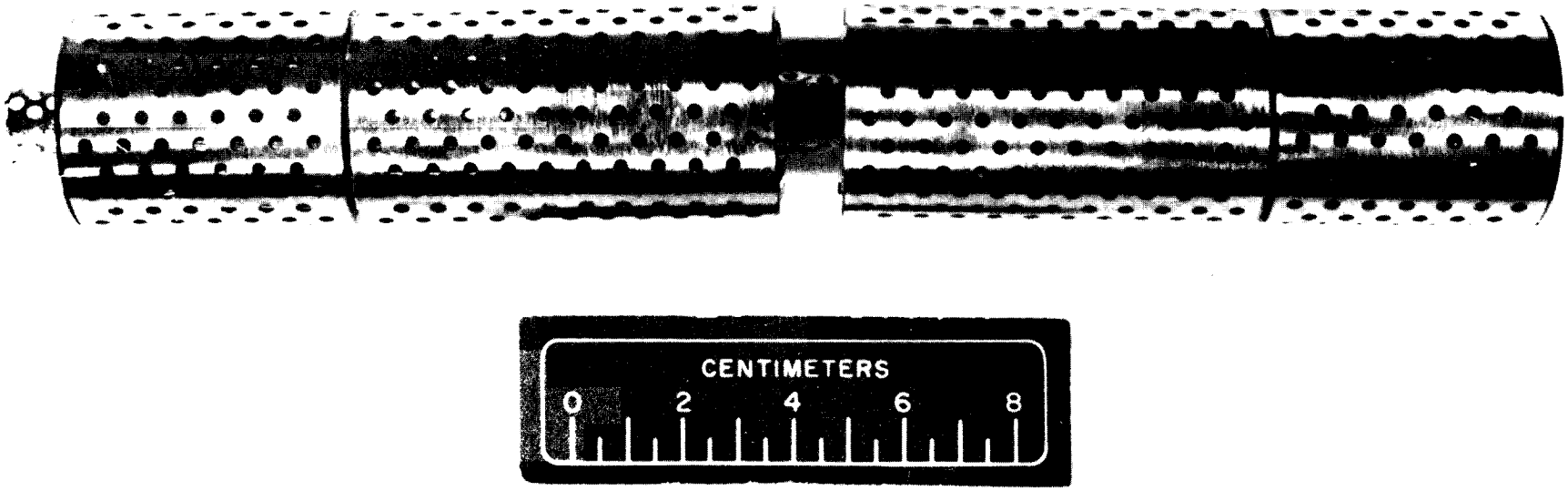

Fig. 3.10. ORR spectral-tailoring capsule MFE-7J specimen assembly.

holders on schedule. Final assembly was so smooth that assembly and facility preparation were completed one reactor cycle ahead of schedule. The experiments were installed in the ORR on June 27, 1985; irradiation began on June 28, the same time as MFE-7J.

3.9 CAPSULE OPERATION

At start-up, the temperatures in the MFE-7J capsule stabilized at 299°C in the 330°C region and at 380°C in the 400°C region, with a control gas composition of 100% helium. The top region of the first capsule was not heated to 330°C so that temperature fluctuations during the cycle due to control rod movements and the effect of the presence of the Heavy Section Steel Technology (HSST) experiments in the production support facility (PSF) could be observed. In the second capsule, average temperatures were 329.1°C in the 330°C region and 394.5°C in the 400°C region. Observing the temperature gradients in the 330 and 400°C regions, it was noted that there was an overlap of temperatures; in the 330°C region there was practically no gradient, whereas in the 400°C region there was a gradient of 10°C/cm. It was then decided to change the operating temperature of the 400°C region to an average of 400°C rather than a maximum of 400°C. This change was initiated on September 20, 1985.

The capsule now operates with a maximum temperature of 330°C in the upper region and an average temperature of 400°C in the lower region. The controlling thermocouples are TE3 in the top region (or TEl, whichever reads the maximum temperature in the region) and TE5 in the lower region, since it is located in the middle of the region.

Capsule MFE-6J achieved the desired temperatures of 60 and 200°C at start-up and has operated as expected.

The neutronics analysis of the MFE-6J and -7J capsules was done by R. A. Lillie of ORNL using flux monitor data obtained by L. R. Greenwood of Argonne National Laboratory. The present operating data of the spectral-tailoring capsules are given in Table 3.20.

4. CONCLUSIONS

The second year of the ORNL-JAERI collaborative testing program in the ORR has been successfully completed. Two HFIR target capsules, JP-1

Table 3.20. Operating data for the ORR-MFE-6J and -7J experimental capsules as of September 30, 1985

	ORR-MFE-6J	ORR-MFE-7J
Insertion date	6/28/85	6/28/85
Exposure, MWh	52,419.8	52,419.8
Equivalent full power days[a]	72.8	72.8
Thermal fluence, neutrons/m^2	1.46 + 25[b]	1.76 + 25
Total fluence, neutrons/m^2	5.03 + 25	6.08 +25
Displacements per atom (dpa)	1.22	1.48
Helium, at. ppm[c]	3.15	4.44

[a]Full power for ORR is 30 MW.

[b]1.46 + 25 is read as 1.46×10^{25}.

[c]Helium and dpa values are for type 316 stainless steel.

and -3, were irradiated beyond 30 dpa, and specimens are being tested. The other six capsules are still being irradiated in the HFIR. The two ORR spectral-tailoring capsules (MFE-6J and -7J) were completed and installed in the core.

The initial test results on U.S. and Japanese PCA alloys and type 316 stainless steel show less than 1% swelling at 30 dpa at temperatures of 300, 400, and 500°C.

Comprehensive microstructural data of JPCA in the SA, 10% CW, and 20% CW conditions, and type 316 stainless steels in the SA and 20% CW conditions reveal that all of the specimens neutron irradiated in HFIR to 30 dpa at 300°C clearly show a high concentration of fine helium bubbles. Also, radiation-produced precipitation of MC was observed in JPCA-20% CW specimens.

The collaborative program has been carried out with a spirit of cooperation and a fine exchange of technical information and ideas that yield great benefits to both the United States and Japan.

5. REFERENCES

1. J. L. Scott et al., *First Annual Progress Report on United States-Japan Collaborative Testing in the High Flux Isotope Reactor and the Oak Ridge Research Reactor for the Period Ending September 30, 1984,* ORNL/TM-9768.

2. P. R. Okamoto and S. D. Harkness, "Stress-Biased Loop Nucleation in Irradiated Type 316 Stainless Steel," *J. Nucl. Mater. 48, 204–6 (1973).*

3. M. L. Grossbeck and K. R. Thoms, "ORR-MFE-4: A Spectral Tailoring Experiment to Simulate the He/dpa Ratio of a Fusion Reactor in Austenitic Stainless Steel," pp. 10-23 in *ADIP Quarterly Progress Report for period Ending June 30, 1980,* DOE/ER-0045/3, U.S. Department of Energy, Office of Fusion Energy.

4. M. L. Grossbeck, "Irradiation Creep in Path A Alloys Irradiated to 5 dpa in the ORR-MFE-4A Spectral Tailoring Experiment," pp. 38-43 in *ADIP Semiann. Prog. Rep. for Period Ending Sept. 30, 1982,* DOE/ER-0045/9, U.S. Department of Energy, Office of Fusion Energy.

5. E. R. Gilbert and B. A. Chin, "In-Reactor Creep Measurements," *Nucl. Technol.* **52,** 273–83 (1961).

6. K. Ehrlich, "Irradiation Creep in Austenitic Stainless Steels," pp. 149-56 in *Mechanical Behavior and Nuclear Applications of Stainless Steel at Elevated Temperatures,* The Metals Society, London, 1982.

BLANK PAGE

ORNL/TM-10102
Distribution
Category UC-20c

INTERNAL DISTRIBUTION

1–2. Central Research Library
3. Document Reference Section
4–5. Laboratory Records Department
6. Laboratory Records, ORNL RC
7. ORNL Patent Section
8. R. G. Alsmiller, Jr.
9. J. Bentley
10. L. A. Berry
11. E. E. Bloom
12. C. K. H. DuBose
13–17. M. L. Grossbeck
18. J. A. Horak
19–23. S. Hamada
24. E. H. Lee
25. K. C. Liu
26. C. G. McKamey
27–31. L. K. Mansur
32. P. J. Maziasz
33. O. B. Morgan
34. D. F. Pedraza
35. C. R. Richmond
36–40. A. F. Rowcliffe
41. M. J. Saltmarsh
42–46. J. L. Scott
47. C. J. Sparks, Jr.
48. R. E. Stoller
49–53. I. I. Siman-Tov
54–56. P. T. Thornton
57–61. K. R. Thoms
62–66. M. P. Tanaka
67. F. W. Wiffen
68. A. Zucker
69. R. J. Charles (Consultant)
70. G. Y. Chin (Consultant)
71. H. E. Cook (Consultant)
72. Alan Lawley (Consultant)
73. W. D. Nix (Consultant)
74. J. C. Williams (Consultant)

EXTERNAL DISTRIBUTION

75–77. HANFORD ENGINEERING DEVELOPMENT LABORATORY, Westinghouse Hanford Company, P.O. Box 1970, Richland, WA 99352

A. M. Ermi, Irradiation Technology, W/A-58
R. W. Powell, Fusion Program, W/A-58
R. J. Puigh, W/A-58

78–88. JAPAN ATOMIC ENERGY RESEARCH INSTITUTE, Tokai Research Establishment, Tokai-mura, Naka-gun, Ibaraki-ken, Japan 319-11

A. Hishinuma, Department of Fuels and Materials Research (5)
S. Jitsukawa, Department of Fuels and Materials Research
T. Kondo, Department of Fuels and Materials Research (5)

89. JAPAN ATOMIC ENERGY RESEARCH INSTITUTE, 2-2, Uchisaiwai-cho, 2-Chome, Chiyoda, Tokyo 100, Japan

E. Shirai

90–93. DOE, OFFICE OF FUSION ENERGY, Washington, DC 20545

M. M. Cohen, ER-533, J-222/GTN
R. J. Dowling, ER-532, J-206/GTN
G. M. Haas, Chief, ER-533, J-213/GTN
T. C. Reuther, ER-533, J-224/GTN

94. DOE, OAK RIDGE OPERATIONS OFFICE, P.O. Box E, Oak Ridge, TN 37831

Office of Assistant Manager for Energy Research and Development

95–258. DOE, TECHNICAL INFORMATION CENTER, Office of Information Services, P.O. Box 62, Oak Ridge, TN 37831

For distribution as shown in DOE/TIC-4500, Distribution Category UC-20c (MFE-Reactor Materials)

☆U.S. GOVERNMENT PRINTING OFFICE 1986–631-056/40041